

Publication No. FHWA-RD-02-078

November 2003

Bottomless Culvert Scour Study: Phase I Laboratory Report



U.S. Department of Transportation

Federal Highway Administration

Research and Development
Turner-Fairbank Highway Research Center
6300 Georgetown Pike
McLean, VA 22101-2296

FOREWORD

The bottomless culvert study described in this report was conducted at the Federal Highway Administration (FHWA) hydraulics laboratory in response to a request by the Maryland State Highway Administration (SHA) in a partnership arrangement in which the Maryland SHA shared the cost of the study. Two suppliers, CONTECH[®] and CONSPAN[®], agreed to provide models of the typical configurations that are used for highway applications. Part of the study objective was to compare results from a simple rectangular shape to the results from shapes that are typically available from the suppliers. This report presents the results of laboratory experiments; it does not represent FHWA policy or endorsement of design concepts. This report is being distributed as an electronic document through the Turner-Fairbank Highway Research Center Web site (www.tfhrcc.gov).

T. Paul Teng, P.E.
Director, Office of Infrastructure
Research and Development

NOTICE

This document is disseminated under the sponsorship of the U.S. Department of Transportation in the interest of information exchange. The U.S. Government assumes no liability for its contents or use thereof. This report does not constitute a standard, specification, policy, or regulation.

The U.S. Government does not endorse products or manufacturers. Trade and manufacturers' names appear in this report only because they are considered essential to the object of the document.

Technical Report Documentation Page

1. Report No. FHWA-RD-02-078		2. Government Accession No.		3. Recipient's Catalog No.	
4. Title and Subtitle BOTTOMLESS CULVERT SCOUR STUDY: PHASE I LABORATORY REPORT				5. Report Date	
				6. Performing Organization Code	
7. Author(s) Kornel Kerenyi, J. Sterling Jones, and Stuart Stein				8. Performing Organization Report No.	
9. Performing Organization Name and Address GKY and Associates, Inc. 5411-E Backlick Road Springfield, VA 22151				10. Work Unit No. (TRAIS)	
				11. Contract or Grant No. DTFH61-95-C-00066	
12. Sponsoring Agency Name and Address Office of Infrastructure Research and Development Federal Highway Administration 6300 Georgetown Pike McLean, VA 22101-2296				13. Type of Report and Period Covered Laboratory Report March 2000-December 2000	
				14. Sponsoring Agency Code	
15. Supplementary Notes Contracting Officer's Technical Representative (COTR): J. Sterling Jones, HRDI-07 The Maryland State Highway Administration (SHA) provided technical assistance and partial funding for this study. Dr. Fred Chang was instrumental in setting up the experimental plan and provided a data analysis strategy. Dr. Xibing Dou provided numerical model results.					
16. Abstract Bottomless culverts are three-sided structures that have sides and a top and use the natural channel for the bottom. As such, they are an environmentally attractive alternative to box, pipe, and pipe arch culvert designs. Bottomless culverts range in size from a few feet to more than 10 meters (35 feet) in width. The failure of such a structure could have severe consequences similar to the failure of a bridge. On the other hand, since the cost of the foundation and scour countermeasures represent a significant portion of the cost of the structure, overdesign of these elements can add significantly to the cost of the project. The Maryland SHA funded a study of scour at bottomless culverts. Several dozen physical modeling configurations were tested and the resulting scour was measured. The results were evaluated and predictive equations for estimating scour depth were developed. These equations will provide guidance for the design of footing depths for bottomless culverts. Additional tests were conducted to determine the riprap sizes needed to prevent the deep scour that was observed near the upstream corners of the culvert when there was substantial approach flow blocked by the roadway embankments. These tests were preliminary and are not an indication that the Federal Highway Administration endorses the concept of using a countermeasure to reduce foundation depth.					
17. Key Words Scour, culverts, hydraulics, physical model.			18. Distribution Statement No restrictions. This document is available to the public through the National Technical Information Service (NTIS), Springfield, VA 22161.		
19. Security Classif. (of this report) Unclassified		20. Security Classif. (of this page) Unclassified		21. No. of Pages 69	22. Price

SI* (MODERN METRIC) CONVERSION FACTORS

APPROXIMATE CONVERSIONS TO SI UNITS

Symbol	When You Know	Multiply By	To Find	Symbol
LENGTH				
in	inches	25.4	millimeters	mm
ft	feet	0.305	meters	m
yd	yards	0.914	meters	m
mi	miles	1.61	kilometers	km
AREA				
in ²	square inches	645.2	square millimeters	mm ²
ft ²	square feet	0.093	square meters	m ²
yd ²	square yard	0.836	square meters	m ²
ac	acres	0.405	hectares	ha
mi ²	square miles	2.59	square kilometers	km ²
VOLUME				
fl oz	fluid ounces	29.57	milliliters	mL
gal	gallons	3.785	liters	L
ft ³	cubic feet	0.028	cubic meters	m ³
yd ³	cubic yards	0.765	cubic meters	m ³
NOTE: volumes greater than 1000 L shall be shown in m ³				
MASS				
oz	ounces	28.35	grams	g
lb	pounds	0.454	kilograms	kg
T	short tons (2000 lb)	0.907	megagrams (or "metric ton")	Mg (or "t")
TEMPERATURE (exact degrees)				
°F	Fahrenheit	5 (F-32)/9 or (F-32)/1.8	Celsius	°C
ILLUMINATION				
fc	foot-candles	10.76	lux	lx
fl	foot-Lamberts	3.426	candela/m ²	cd/m ²
FORCE and PRESSURE or STRESS				
lbf	poundforce	4.45	newtons	N
lbf/in ²	poundforce per square inch	6.89	kilopascals	kPa

APPROXIMATE CONVERSIONS FROM SI UNITS

Symbol	When You Know	Multiply By	To Find	Symbol
LENGTH				
mm	millimeters	0.039	inches	in
m	meters	3.28	feet	ft
m	meters	1.09	yards	yd
km	kilometers	0.621	miles	mi
AREA				
mm ²	square millimeters	0.0016	square inches	in ²
m ²	square meters	10.764	square feet	ft ²
m ²	square meters	1.195	square yards	yd ²
ha	hectares	2.47	acres	ac
km ²	square kilometers	0.386	square miles	mi ²
VOLUME				
mL	milliliters	0.034	fluid ounces	fl oz
L	liters	0.264	gallons	gal
m ³	cubic meters	35.314	cubic feet	ft ³
m ³	cubic meters	1.307	cubic yards	yd ³
MASS				
g	grams	0.035	ounces	oz
kg	kilograms	2.202	pounds	lb
Mg (or "t")	megagrams (or "metric ton")	1.103	short tons (2000 lb)	T
TEMPERATURE (exact degrees)				
°C	Celsius	1.8C+32	Fahrenheit	°F
ILLUMINATION				
lx	lux	0.0929	foot-candles	fc
cd/m ²	candela/m ²	0.2919	foot-Lamberts	fl
FORCE and PRESSURE or STRESS				
N	newtons	0.225	poundforce	lbf
kPa	kilopascals	0.145	poundforce per square inch	lbf/in ²

*SI is the symbol for the International System of Units. Appropriate rounding should be made to comply with Section 4 of ASTM E380.
(Revised March 2003)

TABLE OF CONTENTS

1. INTRODUCTION..... 1

2. EXPERIMENTAL APPROACH 3

TEST FACILITIES AND INSTRUMENTATION 3

 Hydraulic Flume 3

 Electromagnetic Velocity Meter Operation..... 3

 Post-Processing and Data Analysis..... 4

MODEL BOTTOMLESS CULVERT SHAPES 5

EXPERIMENTAL PARAMETERS..... 8

3. THEORETICAL BACKGROUND 11

CALCULATING REPRESENTATIVE VELOCITY 13

 Maryland DOT (Chang) Method for Representative Velocity..... 13

 GKY Method for Representative Velocity 14

NUMERICAL MODEL FOR CALCULATING REPRESENTATIVE VELOCITY 15

CALCULATING CRITICAL VELOCITY 17

 Maryland DOT (Chang) Method for Critical Velocity 17

Niell’s Competent Velocity Concept 17

 GKY Method for Critical Velocity 20

Combined Competent Velocity Curves 23

SCOUR PROTECTION TASK: RIPRAP ANALYSIS 24

4. RESULTS 27

SCOUR RESULTS 27

 Maryland DOT (Chang) Method for Representative Velocity and Critical Velocity 28

 GKY Method for Representative Velocity and Maryland DOT (Chang) Method for Critical Velocity 38

 GKY Method for Representative Velocity and Critical Velocity 42

RIPRAP RESULTS 47

 Maryland DOT (Chang) Method for Representative Velocity..... 47

 GKY Method for Representative Velocity 51

5. CONCLUSIONS 55

6. RECOMMENDED PROCEDURES FOR ESTIMATING MAXIMUM SCOUR FOR BOTTOMLESS CULVERTS..... 57

PROCEDURE USING GKY METHOD FOR REPRESENTATIVE VELOCITY AND SMB EQUATION FOR CRITICAL VELOCITY 57

PROCEDURE USING MARYLAND DOT (CHANG) METHOD FOR REPRESENTATIVE VELOCITY AND CRITICAL VELOCITY..... 59

7. REFERENCES..... 63

LIST OF FIGURES

1.	View of the flume in the Hydraulics Laboratory	3
2.	Example of a front panel	4
3.	Example of a block diagram	5
4.	Rectangular model, vertical face	6
5.	Rectangular model with wingwalls	6
6.	CONSPAN model.....	7
7.	CONSPAN model with wingwalls	7
8.	CONTECH model.....	8
9.	Rectangular model from the scour protection task	9
10.	Flow concentration and separation zone	11
11(a).	Definition sketch prior to scour	12
11(b).	Definition sketch after scour	12
11(c).	Definition sketch for blocked area.....	12
12.	Chang's resultant velocity location	14
13.	GKY's resultant velocity approach.....	15
14.	Velocity locations for 2D model.....	16
15.	Resultant velocity comparison with numerical model at location 2.....	16
16.	Comparison of Chang's and GKY's resultant velocities.....	17
17.	Competent velocity curves for the design of waterway openings in scour backwater conditions (from Niell).....	18
18.	Chang's approximations	20
19.	Shields parameter as a function of the particle Reynolds number	21
20.	Combined competent velocity curves for a flow depth of 3 m (10 ft).....	23
21.	Combined competent velocity curves for a flow depth of 0.3 m (1.0 ft).....	24
22.	Post-processing: Data analysis flow chart	27
23.	Maryland DOT's (Chang's) resultant velocity with Chang's approximation equation and local scour ratio as a function of the Froude number, using a linear regression	28
24.	Measured and computed data with and without wingwalls.....	29
25.	Maryland DOT's (Chang's) resultant velocity with Chang's approximation equation for critical velocity and local scour ratio as a function of the Froude number, using a second order regression	30
26.	Measured and computed data with and without wingwalls.....	30
27.	Maryland DOT's (Chang's) resultant velocity with Chang's approximation for critical velocity and local scour ratio as a function of the Froude number, using a linear regression.....	31
28.	Measured and computed data with and without wingwalls.....	32
29.	Maryland DOT's (Chang's) resultant velocity with Chang's approximation for critical velocity and local scour ratio as a function of the blocked area over the squared flow depth	33
30.	Measured and computed data with and without wingwalls.....	33
31.	Maryland DOT's (Chang's) resultant velocity with Chang's approximation for critical velocity and local scour ratio as a function of the blocked area over the squared computed equilibrium depth.....	34
32.	Measured and computed data with and without wingwalls.....	35

33.	Maryland DOT's (Chang's) resultant velocity with Chang's approximation equation and local scour ratio as a function of the blocked discharge normalized by the acceleration of gravity (g) and the computed equilibrium depth	36
34.	Measured and computed data with and without wingwalls.....	36
35.	GKY's resultant velocity with Chang's approximation equation for critical velocity and local scour ratio as a function of the blocked area over the squared flow depth	39
36.	Measured and computed data with and without wingwalls.....	39
37.	GKY's resultant velocity with Chang's approximation equation for critical velocity and local scour ratio as a function of the blocked area over the squared computed equilibrium depth.....	40
38.	Measured and computed data with and without wingwalls.....	41
39.	GKY's resultant velocity with the SMB equation for critical velocity and local scour ratio as a function of the blocked area over the squared flow depth.....	42
40.	Measured and computed data with and without wingwalls.....	43
41.	GKY's resultant velocity with the SMB equation for critical velocity and local scour ratio as a function of the blocked area over the squared computed equilibrium depth.....	44
42.	Measured and computed data with and without wingwalls.....	44
43.	GKY's resultant velocity with the SMB equation for critical velocity and local scour ratio as a function of the blocked discharge normalized by the acceleration of gravity (g) and the computed equilibrium depth.....	45
44.	Measured and computed data with and without wingwalls.....	46
45.	Maryland DOT's (Chang's) resultant velocity and stable riprap size from the Ishbash equation with the blocked area over the squared flow depth as the independent regression variable.....	48
46.	Measured and computed data.....	48
47.	Maryland DOT's (Chang's) resultant velocity and stable riprap size from the Ishbash equation with the blocked discharge normalized by the acceleration of gravity (g) and the flow depth as the independent regression variable	49
48.	Measured and computed data.....	50
49.	GKY's resultant velocity and stable riprap size from the Ishbash equation with the blocked area over the squared flow depth as the independent regression variable.....	51
50.	Measured and computed data.....	52
51.	GKY's resultant velocity and stable riprap size from the Ishbash equation with the blocked discharge normalized by the acceleration of gravity (g) and the flow depth as the independent regression variable	53
52.	Measured and computed data.....	53

LIST OF TABLES

1.	Independent regression variables and R^2 values using the Maryland DOT (Chang) method.....	38
2.	Independent regression variables and R^2 values using the GKY and Maryland DOT (Chang) methods	41
3.	Independent regression variables and R^2 values using the GKY method for representative velocity and critical velocity	47
4.	Independent regression variables and R^2 values using the Maryland DOT (Chang) method for representative velocity	50
5.	Independent regression variables and R^2 values using the GKY method for representative velocity	54

LIST OF ACRONYMS AND ABBREVIATIONS

AASHTO	American Association of State Highway and Transportation Officials
COTR	Contracting Officer's Technical Representative
DOT	Department of Transportation
FHWA	Federal Highway Administration
MSE	Mean Square Error
NTIS	National Technical Information Service
RSQ	Correlation Coefficient
R^2	Correlation Coefficient
SG	Specific Gravity
SHA	State Highway Administration
SI	International System of Units (metric system)
SMB	Shields, Manning, and Blodgett
TFHRC	Turner-Fairbank Highway Research Center
V_C	Critical Velocity
VI	Virtual Instruments
V_R	Representative Velocity
W.S.	Water Surface

1. INTRODUCTION

Bottomless (or three-sided) culverts use the natural channel bed and are environmentally attractive alternatives to traditional closed culverts. Moreover, they are considered by many highway agencies to be economical alternatives for replacing short bridges. They are typically placed on spread footings, and the issue of scour and the depth of footing must be addressed. The scour problem is analogous to abutment and contraction scour in a bridge opening and can be treated in much the same manner.

The study described in this report was conducted at the Federal Highway Administration's (FHWA) Hydraulic Laboratory at the request of the Maryland State Highway Administration (SHA) in a partnership arrangement in which the Maryland SHA shared the cost of the study. Two suppliers, CONTECH[®] and CONSPAN[®], agreed to provide models of the typical configurations used for highway applications. Part of the study objective was to compare the results from a simple rectangular shape to the results from shapes that are typically available from the suppliers.

Since abutment scour estimates at bridge openings are often quite large, a scour protection task was included to determine the sizes of rock riprap that might be required to reduce scour in the most critical zones.

A major consideration in estimating scour and riprap sizes is the flow distribution at the entrance of the culvert, especially when there is side flow that is being contracted to pass through the opening. Although the analysis was aimed at simple one-dimensional (1D) approximations for this flow distribution, some 2D numerical simulations of the laboratory experiments were conducted to demonstrate how this could be used if they are available to a designer. As numerical models become user-friendly and computers become more powerful, 2D and even 3D numerical results are likely to become readily available to designers.

In presenting status reports to drainage engineers at American Association of State Highway and Transportation Officials (AASHTO) meetings and at hydraulic conferences, we found that there was widespread interest in this topic. This report is an attempt to share the results of this study with a larger audience.

2. EXPERIMENTAL APPROACH

TEST FACILITIES AND INSTRUMENTATION

The experiments were conducted in the FHWA Hydraulics Laboratory located at the Turner-Fairbank Highway Research Center (TFHRC) in McLean, VA. Test facilities and instrumentation used during the experiments are described in this section.



Figure 1. View of the flume in the Hydraulics Laboratory.

Hydraulic Flume

The experiments were completed in a 21.34-meter- (m) long by 1.83-m-wide (70-foot- (ft) long by 6-ft-wide) rectangular flume with a 2.4-m-long by 1.83-m-wide (8-ft-long by 6-ft-wide) recessed section to allow for scour hole formation. A 9.14-m (30-ft) flow development section from the head box to the transition section consisted of a plywood floor constructed 0.1 m (4 inches) above the stainless steel flume bottom. The plywood floor was coated with a layer of epoxy paint and sand to approximate the roughness of the sand bed channel in the recessed section. The walls of the flume are made of a smooth glass. The flume was set at a constant slope of 0.04 percent and the depth of flow was controlled with an adjustable tailgate located at the downstream end of the flume. Flow was supplied by a 0.3-cubic meter/second (m^3/s) (10-cubic foot/second (ft^3/s)) pumping system. The discharge was measured with an electromagnetic flow meter.

Electromagnetic Velocity Meter Operation

A 13-millimeter (mm) spherical electromagnetic velocity sensor (Marsh-McBirney 523) was used to measure equivalent two-directional mean velocities in a plane parallel to the flume bed.

A fluctuating magnetic field was produced in the fluid surrounding the spherical sensor that was orthogonal to the plane of four carbon-tipped electrodes. As a conductive fluid passed around the sensor, an electric potential was produced proportional to the product of the fluid velocity component tangent to the surface of the sphere and normal to the magnetic field and the magnetic field strength. The electrodes located at four locations on the sensor detected the voltage potential created by the flowing water. The voltage potential produced was proportional to the velocity of the fluid flowing in the plane of the electrodes. Two orthogonal velocity components in the plane of the electrodes were measured. Detailed information on the meter operation is available in the technical manual, [Instruction Manual Model 511 Electromagnetic Water Current Meter](#), provided by the probe manufacturer, [Marsh-McBirney Inc.](#)

Post-Processing and Data Analysis

Post-processing and data analysis were performed using the LabVIEW™ graphical programming technique for building applications such as testing and measurement, data acquisition, instrument control, data logging, measurement analysis, and report generation. LabVIEW programs are called virtual instruments (VI's) because their appearance and operation imitate physical instruments such as oscilloscopes and multimeters. Every VI uses functions that manipulate input from the user interface or other sources and displays that information or moves it to other files or other computers.

A VI contains the following three components:

- Front panel: Serves as the user interface (figure 2).
- Block diagram: Contains the graphical source code that defines the functionality of the VI (figure 3).
- Icon and connector pane: Identifies the VI so that you can use one VI in another VI. A VI within another VI is called a subVI. A subVI corresponds to a subroutine in text-based programming languages.

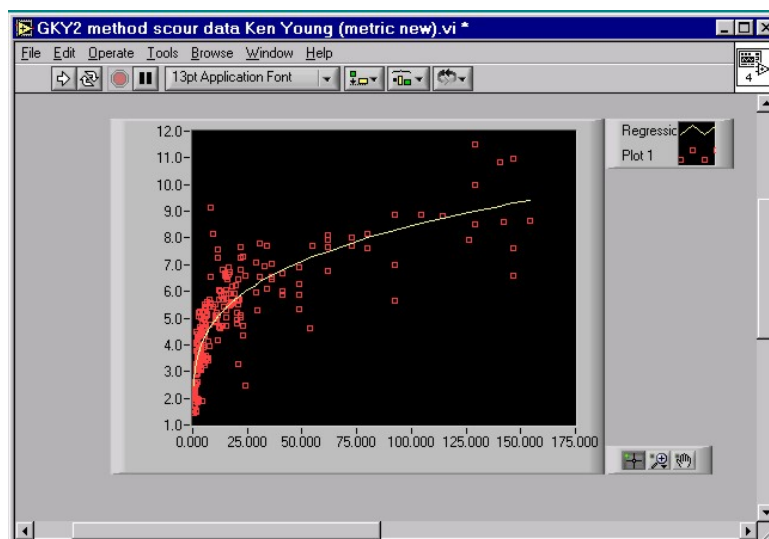


Figure 2. Example of a front panel.

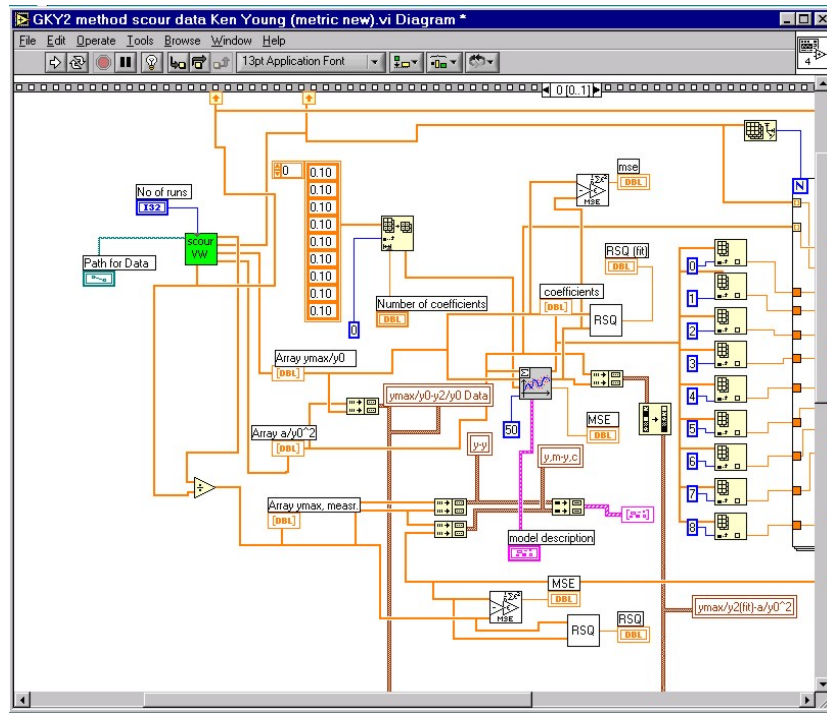


Figure 3. Example of a block diagram.

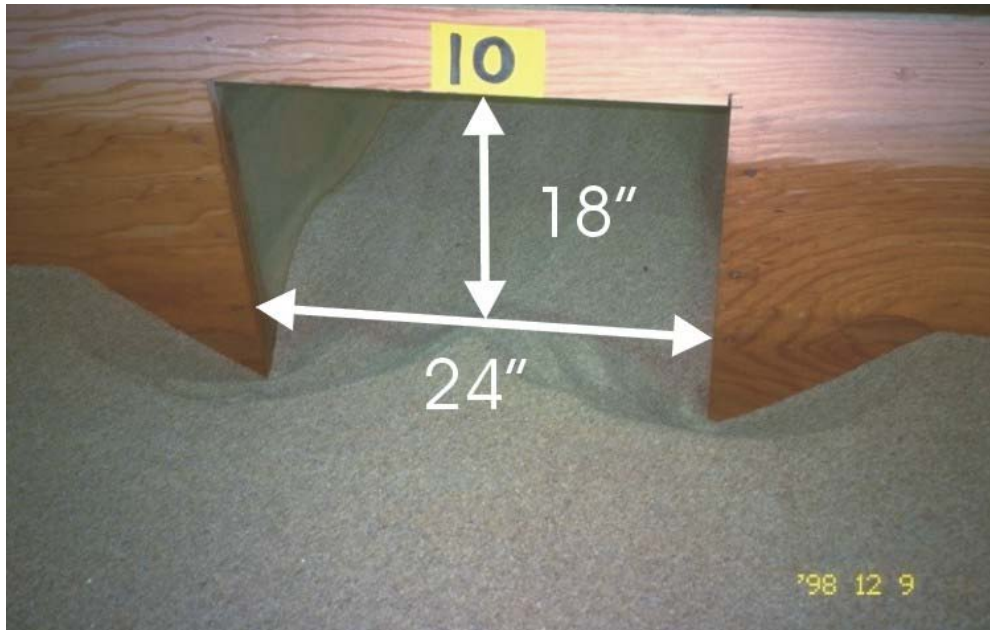
The regression analysis was done using the nonlinear Levenberg-Marquardt fit algorithm to determine the set of coefficients that minimize the chi-square quantity:

$$\chi^2 = \sum_{i=0}^{N-1} \left(\frac{y_i - f(x_i; a_1, \dots, a_M)}{\sigma_i} \right)^2 \quad (1)$$

In this equation, x_i and y_i are the input data points, and $f(x_i; a_1, \dots, a_M)$ is the nonlinear function, where a_1, \dots, a_M are coefficients. If the measurement errors are independent and normally distributed with a constant standard deviation $\sigma_i = \sigma$, this is also the least-square estimation.

MODEL BOTTOMLESS CULVERT SHAPES

Three bottomless culvert shapes were constructed and tested: (1) a rectangular model with a width of 0.61 m (2 ft) and a height of 0.46 m (1.5 ft) (figure 4), (2) a CONSPAN model with a width of 0.61 m and a height of 0.45 m (1.46 ft) (figure 6), and (3) a CONTECH model with a width of 0.61 m and a height of 0.42 m (1.36 ft) (figure 8). All three models were evaluated with 45-degree wingwalls (figures 5 and 7) and without wingwalls. The models were constructed of Plexiglas®. Marine plywood was used for the vertical face of the models and for the wingwalls. The models were mounted in the centerline of the flume.

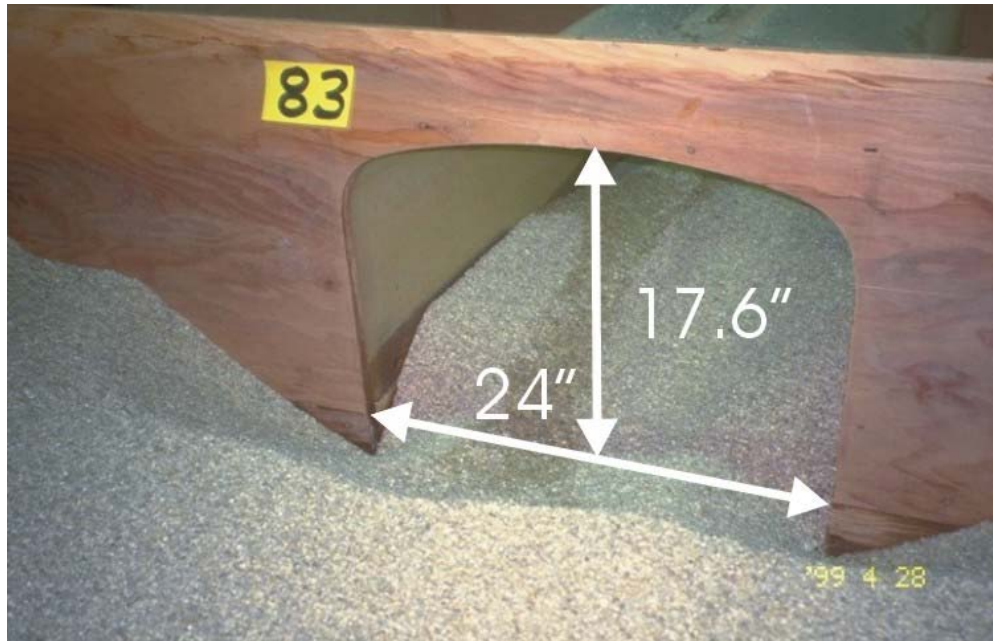


1 inch = 25.4 mm

Figure 4. Rectangular model, vertical face.



Figure 5. Rectangular model with wingwalls.

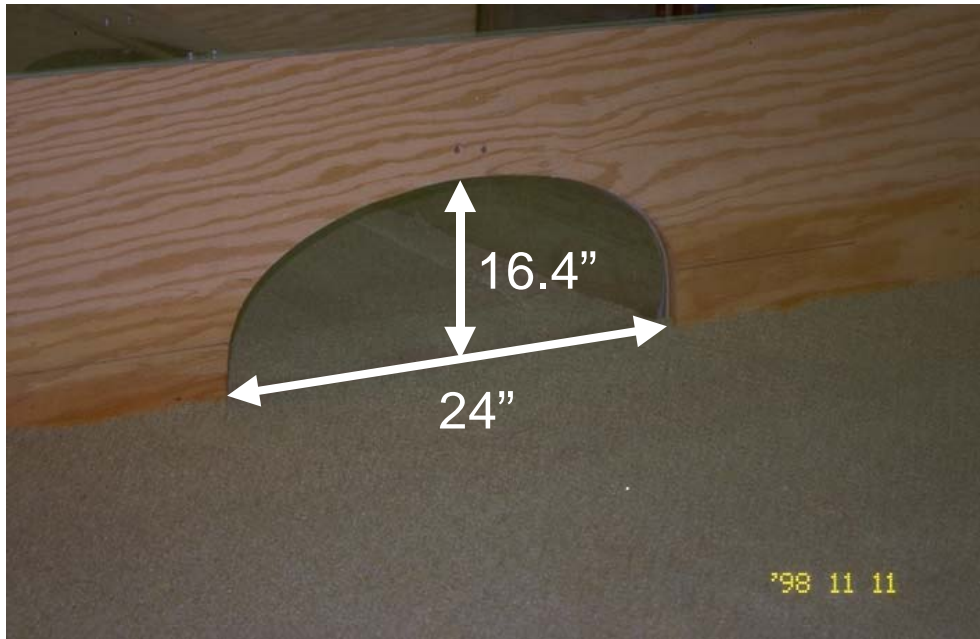


1 inch = 25.4 mm

Figure 6. CONSPAN model.



Figure 7. CONSPAN model with wingwalls.



1 inch = 25.4 mm

Figure 8. CONTECH model.

EXPERIMENTAL PARAMETERS

Steady flow experiments were conducted for approach flow depths of 0.106 m, 0.212 m, and 0.304 m (0.35 ft, 0.7 ft, and 1 ft) and approach velocities ranging from 0.091 to 0.304 m/s (0.3 to 1 ft/s). The discharges to obtain the approach flow conditions varied from approximately 0.019 to 0.14 m³/s (0.7 to 5 ft³/s). The particle size (D_{50}) was varied from 1.2 to 3.0 mm (0.004 to 0.01 ft) for the scour experiments.

Riprap experiments were conducted for uniform particle sizes of 9.5 mm, 12.7 mm, 20.3 mm, and 25 mm (0.375 inch, 0.5 inch, 0.8 inch, and 1 inch). The velocity was increased incrementally until discernible areas of particles were dislodged, which was considered to define the failure condition for that particle size. Because of time constraints, riprap experiments (figure 9) were conducted for the rectangular model with vertical headwalls only. Vertical headwalls were considered a worst-case condition and wingwalls should reduce the riprap size determined from these experiments.



Figure 9. Rectangular model from the scour protection task.

3. THEORETICAL BACKGROUND

As the photographs in the previous section illustrate, the scour was always deepest near the corners at the upstream entrance to the culvert. This observation is attributed, in part, to the concentration of flow near the upstream corners as the flow that is being blocked by the embankments is contracted and forced to go through the culvert opening. However, it is also attributed to the vortices and strong turbulence generated in the flow separation zone as the blocked flow mixes with the main channel flow at the upstream end of the culvert (figure 10). It is much like the abutment scour phenomenon that researchers have observed for bridge scour models.

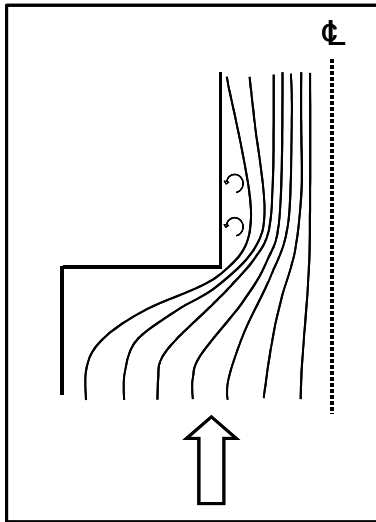


Figure 10. Flow concentration and separation zone.

Several researchers, including Chang,⁽¹⁾ GKY and Associates, Inc.,⁽²⁾ and Sturm,⁽³⁾ have suggested that bridge abutment scour can be analyzed as a form of flow distribution scour by incorporating an empirical adjustment factor to account for vorticity and turbulence. The equilibrium flow depth required to balance the sediment load into and out of the scour zone for the assumed flow distribution can be determined analytically. The adjustment factor to account for vorticity and turbulence can be derived from laboratory results. These notions were used to formulate the theoretical background for analyzing the culvert scour data. Variables used in the data analysis are illustrated in the definition sketches (figures 11(a) through 11(c)).

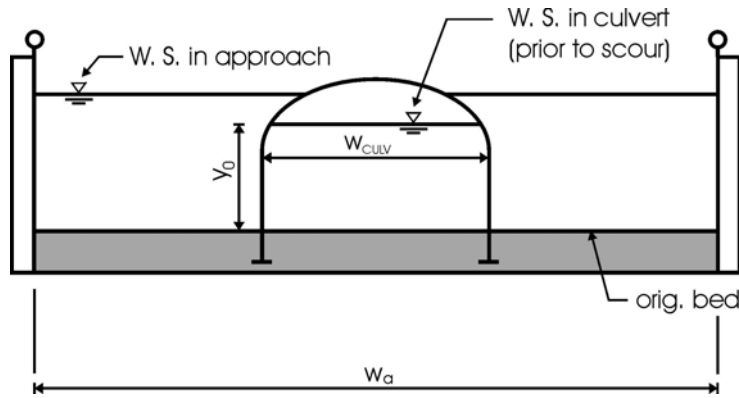


Figure 11(a). Definition sketch prior to scour.

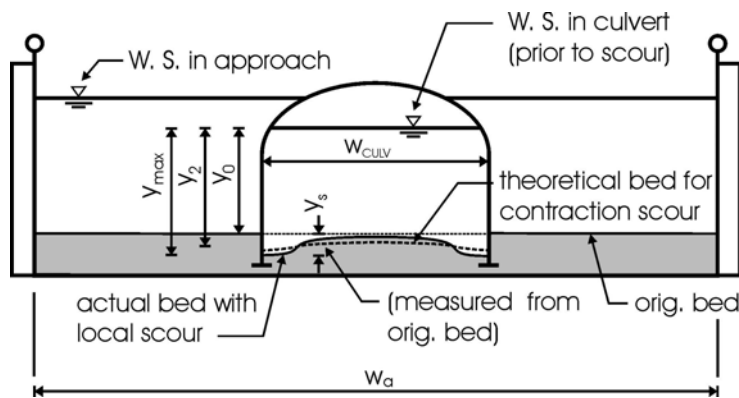


Figure 11(b). Definition sketch after scour.

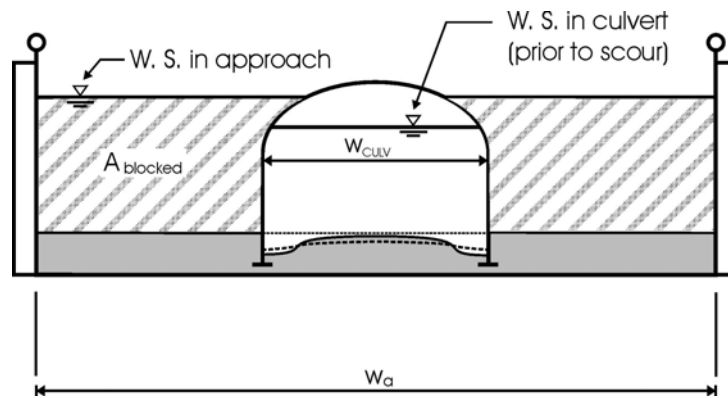


Figure 11(c). Definition sketch for blocked area.

Equation 2 is an expression for the unit discharge for an assumed flow distribution remaining constant as the scour hole develops. If no sediment is being transported into the scour hole, as was the case with all of our experiments, then no sediment can be transported out of the scour hole at equilibrium. In this case, the velocity must be reduced to the critical incipient motion velocity for the sediment size at the equilibrium flow depth (y_2). This equation forms the basis for the analysis:

$$V_R y_0 = V_C y_2 \quad (2)$$

where:

$V_{RY0} = q_R =$ the assumed representative unit discharge across the scour hole at the beginning of scour

The above equation can be rearranged to yield an equilibrium flow depth (y_2) after the representative velocity (V_R) at the beginning of scour and the critical incipient motion velocity (V_C) are determined. This equilibrium depth reflects the scour that is attributed to the flow distribution. The measured maximum depth at the corners of the culvert was always greater than the computed equilibrium depth. An empirical coefficient (K_{ADJ}), defined by equation 3, was needed to explain the extra scour depths. The laboratory data and regression analyses were used to derive an expression for this coefficient.

$$K_{ADJ} = \frac{y_{max}}{y_2} \quad (3)$$

Several different independent variables were tried to derive the expression for K_{ADJ} ; however, what seemed to work best for this data was the blocked discharge ($Q_{blocked}$) normalized by the acceleration of gravity (g) and the computed equilibrium depth (y_2) as formulated in equation 4:

$$K_{ADJ} = f \left(\frac{Q_{blocked}}{\sqrt{g} * y_2^{5/2}} \right) \quad (4)$$

$Q_{blocked}$ is the portion of the approach flow to one side of the channel centerline that is blocked by the embankment as the flow approaches the culvert.

The literature describes several methods for determining an approximation for representative velocity and critical velocity. Methods described by Chang and by GKY were tried in various combinations to determine which worked best for this data. These methods are discussed below.

CALCULATING REPRESENTATIVE VELOCITY

Maryland DOT (Chang) Method for Representative Velocity

Chang, through his work for the Maryland SHA, developed equations 5 and 6 to calculate the resultant velocity based on potential flow assumptions at a distance equal to one-tenth of the length of the blocked flow (figure 12):

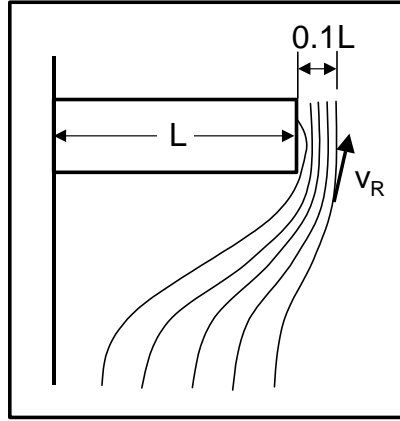


Figure 12. Chang's resultant velocity location.

$$V_R = K_V \left[\frac{Q}{A_{opening}} \right] \quad (5)$$

$$K_V = 1 + 0.8 \left(\frac{w_{opening}}{w_a} \right)^{1.5} \quad (6)$$

where:

- K_V = velocity coefficient to account for flow concentration where side flow converges with main channel flow based on potential flow assumptions
- Q = total discharge through the culvert, ft^3/s
- $A_{opening}$ = average flow area within the culvert, ft^2
- $w_{opening}$ = average flow width in the culvert, ft
- w_a = width of flow in the approach section, ft

These equations are dimensionally homogeneous and are independent of the system of units as long as they are consistent.

GKY Method for Representative Velocity

GKY describes representative velocity across the scour hole as the resultant of the lateral and longitudinal velocity components as shown in equations 7, 8, and 9.

Applying the Pythagorean theorem yields:

$$V_R = \sqrt{V_x^2 + V_y^2} \quad (7)$$

with

$$V_x = \frac{Q}{A_{opening}} \quad (8)$$

and

$$V_y = \frac{Q_{blocked}}{0.43 A_a} \quad (9)$$

It should be noted that equation 9 above is an unpublished modification of the method published by Young, et al.⁽²⁾; however, the basic concept is similar to the published version.

For the simple rectangular cross section used for the flume experiments, $Q_{blocked}$ could be estimated from equation 10:

$$Q_{blocked} = Q \frac{A_{blocked}}{A_a} \quad (10)$$

where:

- V_x = velocity in the flow direction, ft/s (figure 13)
- V_y = velocity orthogonal to the flow direction, ft/s
- $Q_{blocked}$ = approach flow blocked by the embankment on one side of the channel, ft³/s
- A_a = total approach flow area on one side of the channel, ft²
- $A_{blocked}$ = approach flow area that is blocked by the embankments on one side of the channel, ft²

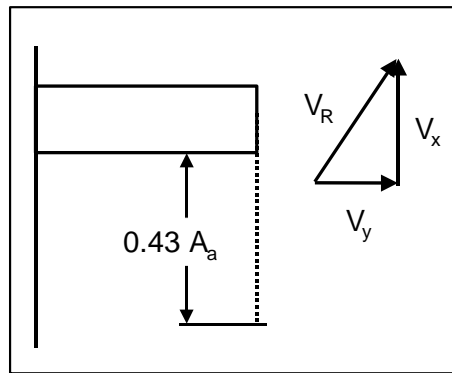
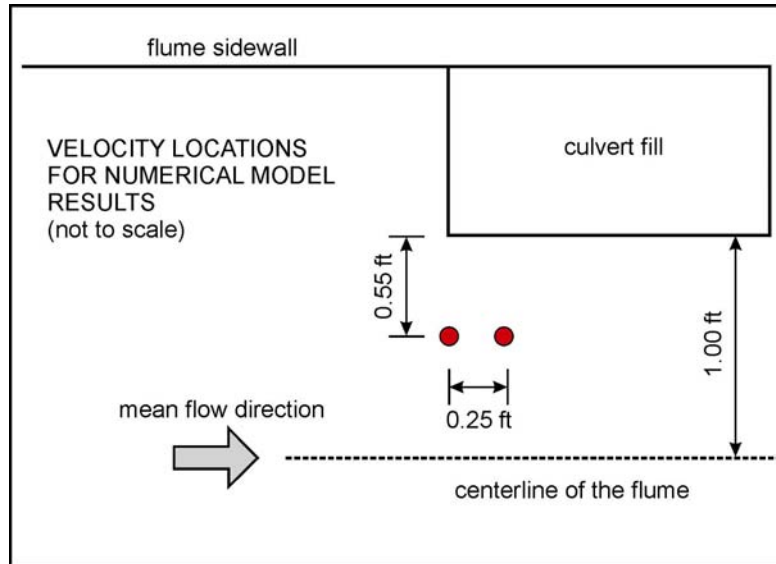


Figure 13. GKY's resultant velocity approach.

NUMERICAL MODEL FOR CALCULATING REPRESENTATIVE VELOCITY

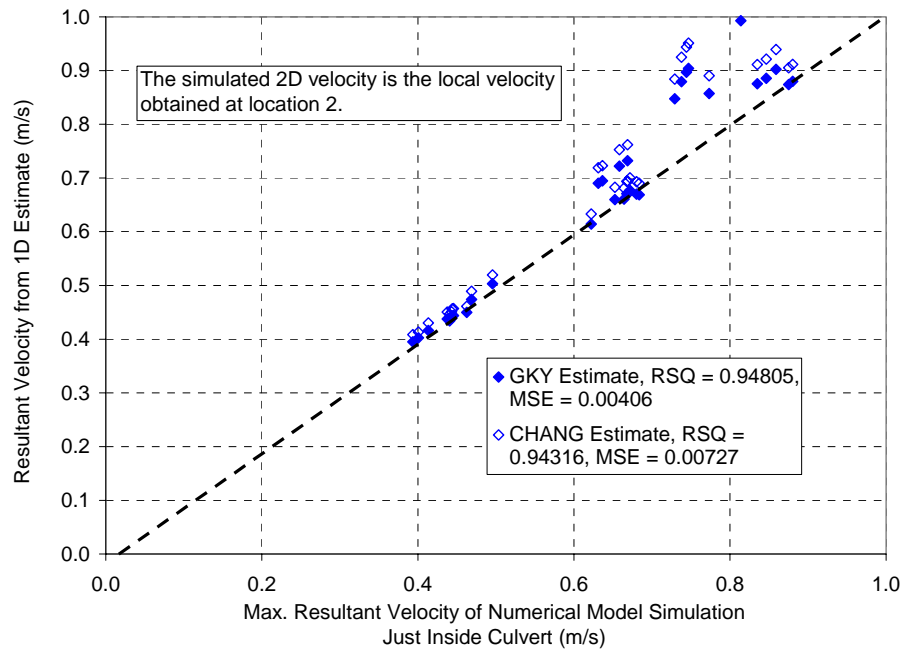
Since some designers probably have access to 2D numerical models, they will not necessarily need to rely on the 1D approximations for representative velocity to be used in the computations. Xibing Dou simulated the laboratory experiments with a 2D numerical model. This model uses the Finite Element Surface-Water Modeling System: Two-Dimensional Flow in a Horizontal Plane (FESWMS-2DH) program to solve the hydrodynamic equations that describe 2D flow in the horizontal plane. The effects of bed friction and turbulent stresses are considered and water column pressure is hydrostatic. The estimation of representative velocity uses the average x and y element velocities (\bar{V}_x and \bar{V}_y) for the element transect aligned with the upstream face, excluding the element at the corner and including the next three elements. The numerical model gave rapidly varying velocities in the vicinity of the corners of the culverts. Chang faced a

similar problem in interpreting the velocities based on potential flow transformations. Dou tried Chang's selection of a depth-averaged velocity at a distance that was 10 percent of the embankment length into the main channel as illustrated in figure 12, but found better agreement with the 1D approximations by using two locations in a zone that was approximately 10 percent of the culvert width downstream of the culvert face and 25 percent of the culvert width from the culvert wall (figure 14).



1 ft = 0.305 m

Figure 14. Velocity locations for 2D model.



RSQ = R^2 = correlation coefficient
MSE = mean square error

Figure 15. Resultant velocity comparison with numerical model at location 2.

Figure 15 is a comparison of the 2D numerical model results with the 1D approximations suggested by Chang and GKY. The 1D approximations are consistently higher than the numerical results, which is interpreted to mean that the 1D approximations are conservative. Numerical model results could underpredict scour if they are used with empirical equations based on 1D approximations; however, the differences are probably insignificant compared to the differences in the ideal conditions tested in the flume and the conditions that are in a natural channel. In addition to the previous comparison between numerical and 1D measurements, figure 16 shows the comparison between Chang’s resultant velocity and GKY’s resultant velocity.

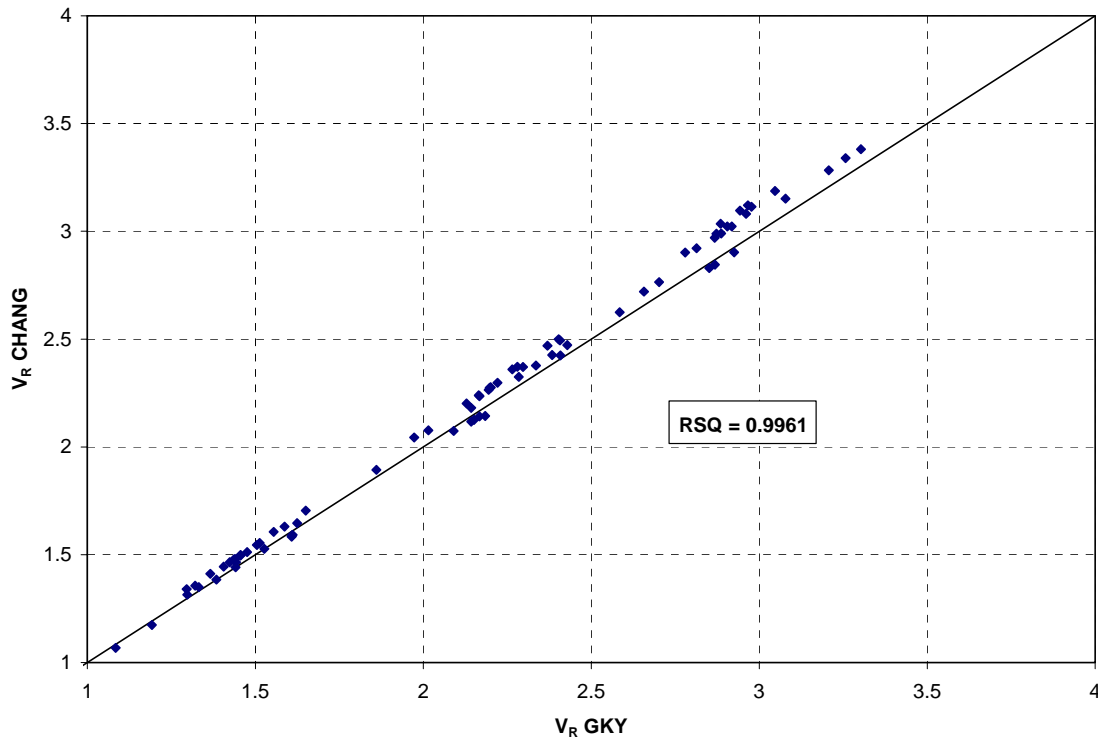


Figure 16. Comparison of Chang’s and GKY’s resultant velocities.

CALCULATING CRITICAL VELOCITY

Maryland DOT (Chang) Method for Critical Velocity

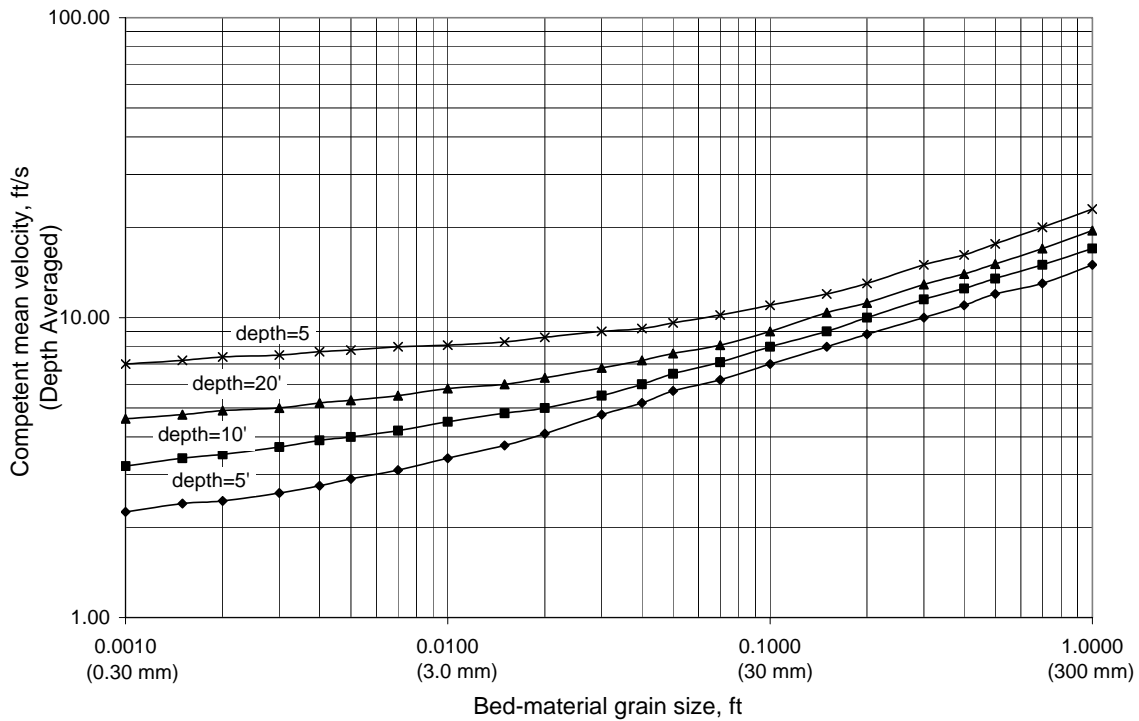
Chang uses Niell’s⁽⁴⁾ competent velocity curves to calculate critical velocity. Niell presents a set of competent (critical) velocity curves based on flow depth, velocity, and the size of the bed material. Niell’s curves are derived from the Shields curve using varying Shields numbers for different particle sizes. To facilitate doing computations on a computer spreadsheet, Chang⁽²⁾ derived a set of simplified equations that represent Niell’s curves quite well.

Niell’s Competent Velocity Concept

Niell’s competent velocity is comparable in its definition to the critical flow velocity for causing incipient motion of bed materials. The equations by Laursen and Niell for computing critical velocity (presented in FHWA’s Hydraulic Engineering Circular 18 (HEC-18)) are generally applicable for particles of bed material larger than 0.03 m (0.1 ft). For bed material smaller than

this size, these equations can be expected to underestimate critical velocity. Niell developed a series of curves for determining the critical velocity for particles smaller than 0.03 m based on the Shields curve.

Chang transformed the plots of Niell's curves (figure 17) into a set of equations for computing critical velocity based on the flow depth and the median diameter of the particle. These equations are set forth below.



1 ft = 0.305 m

Figure 17. Competent velocity curves for the design of waterway openings in scour backwater conditions (from Niell).⁽⁴⁾

- For $D_{50} > 0.03$ m (0.1 ft)

$$V_C = K_U 11.5 y_2^{1/6} D_{50}^{1/3} \quad (11)$$

where:

- y_2 = equilibrium flow depth, m or ft
- D_{50} = sediment size, m or ft
- K_U = 0.55217 for the International System of Units (SI) (metric system) or 1.0 for U.S. customary units

- For 0.03 m (0.1 ft) $> D_{50} > 0.0003$ m (0.001 ft)

$$V_C = K_{U1} 11.5 y_2^x D_{50}^{0.35} \quad (12)$$

The exponent x is calculated using equation 13:

$$x = K_{U2} \frac{0.123}{D_{50}^{0.20}} \quad (13)$$

where:

y_2	=	equilibrium flow depth, m or ft
D_{50}	=	sediment size, m or ft
K_{U1}	=	$0.3048^{(0.65-x)}$ for SI units or 1.0 for U.S. customary units
x	=	exponent from equation 13
K_{U2}	=	0.788 for SI units or 1.0 for U.S. customary units

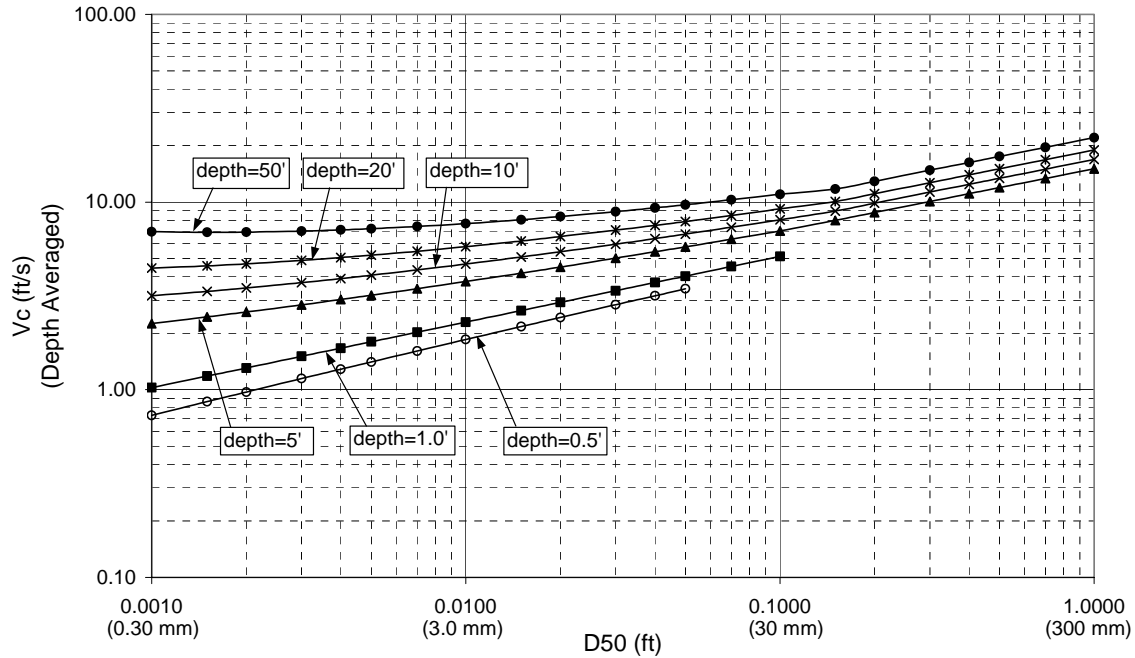
- For $0.0003 \text{ m (0.001 ft)} > D_{50}$

$$V_c = K_U \sqrt{y_2} \quad (14)$$

where:

y_2	=	equilibrium flow depth, m or ft
D_{50}	=	sediment size, m or ft
K_U	=	0.55217 for SI units or 1.0 for U.S. customary units

Chang's equations are plotted in figure 18. Niell's competent velocity curves are intended for field conditions with flow depths of 1.5 m (5 ft) or greater. Chang's equations were extrapolated to flow depths below 0.30 m for these experiments and to curves for flow depths of 0.305 and 0.15 m (1 and 0.5 ft) (figure 18). Our sediment sizes fell in a range that could be described by equations 12 and 13.



1 ft = 0.305 m

Figure 18. Chang's approximations.

GKY Method for Critical Velocity

The GKY method combines the Shields,⁽⁵⁾ Manning,⁽⁶⁾ and Blodgett⁽⁷⁾ (SMB) equations to calculate critical velocity. The starting equation is the average shear stress in a control volume of flow:

$$\tau = \gamma y_2 S_F \tag{15}$$

Experimental observations highlighted the importance of the Shields parameter (SP), which is defined as:

$$SP = \frac{\tau_c}{(\gamma_s - \gamma) D_{50}} \tag{16}$$

The critical value of the stability parameter may be defined at the inception of bed motion, i.e., $SP = (SP)_C = 0.047$. Shields showed that $(SP)_C$ is primarily a function of the shear Reynolds number (figure 19).

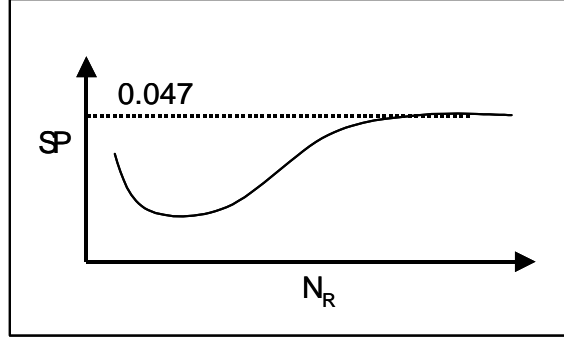


Figure 19. Shields parameter as a function of the particle Reynolds number.

Rearranging equation 16, inserting $(SP)_c = 0.047$, and setting τ from equation 14 equal to τ_c from equation 15 leads to:

$$0.047(\gamma_s - \gamma)D_{50} = \gamma y_2 S_F \quad (17)$$

Rearranging Manning's equation to compute the friction slope leads to:

$$S_F = \frac{V^2 n^2}{K_{UM}^2 y_2^{4/3}} \quad (18)$$

where:

$$K_{UM} = \begin{array}{l} 1.0 \text{ for SI units or} \\ 1.49 \text{ for U.S. customary units} \end{array}$$

Substituting equation 18 for S_F in equation 17 results in:

$$0.047(\gamma_s - \gamma)D_{50} = \frac{\gamma y_2 V_c^2 n^2}{K_{UM}^2 y_2^{4/3}} \quad (19)$$

This may be simplified by consolidating the specific weight (γ) terms and the y_2 terms:

$$0.047\left(\frac{\gamma_s}{\gamma} - 1\right)D_{50} = \frac{V_c^2 n^2}{K_{UM}^2 y_2^{1/3}} \quad (20)$$

Note that:

$$\frac{\gamma_s}{\gamma} = S.G. \text{ (no units)} \quad (21)$$

Sand such as that used in these experiments is considered to have a specific gravity (SG) of 2.65. Substituting this into equation 20 and rearranging to isolate V_c^2 leads to:

$$\frac{0.047(1.65)D_{50}y_2^{1/3}K_{UM}^2}{n^2} = V_c^2 \quad (22)$$

The square root of equation 22 gives the equation for computing critical velocity:

$$V_c = \frac{K_{UM}0.28D_{50}^{1/2}y_2^{1/6}}{n} \quad (23)$$

Blodgett's equations for average estimates of Manning's n for sand- and gravel-bed channels follow. Equation 25 applies for the depths and sand particle sizes used in our experiments.

$$n = \frac{K_{UB}0.525 y_2^{1/6}}{\sqrt{g} \left[0.794 + 1.85 \text{Log} \left(\frac{y_2}{D_{50}} \right) \right]} \quad \text{for } 1.5 < \frac{y_2}{D_{50}} < 185 \quad (24)$$

$$n = \frac{K_{UB}0.105 y_2^{1/6}}{\sqrt{g}} \quad \text{for } 185 < \frac{y_2}{D_{50}} < 30,000 \quad (25)$$

Where: g = acceleration of gravity
 = 9.81 m/s² for SI units
 = 32.2 ft/s² for U.S. customary units

K_{UB} = 1/1.49 for SI units
 = 1.0 for U.S. customary units

Substituting equation 25 for n in equation 23 and then simplifying leads to:

$$V_c = \frac{K_{UM}0.28D_{50}^{1/2}y_2^{1/6}}{K_{UB} \left(\frac{0.105 y_2^{1/6}}{\sqrt{g}} \right)} \quad (26)$$

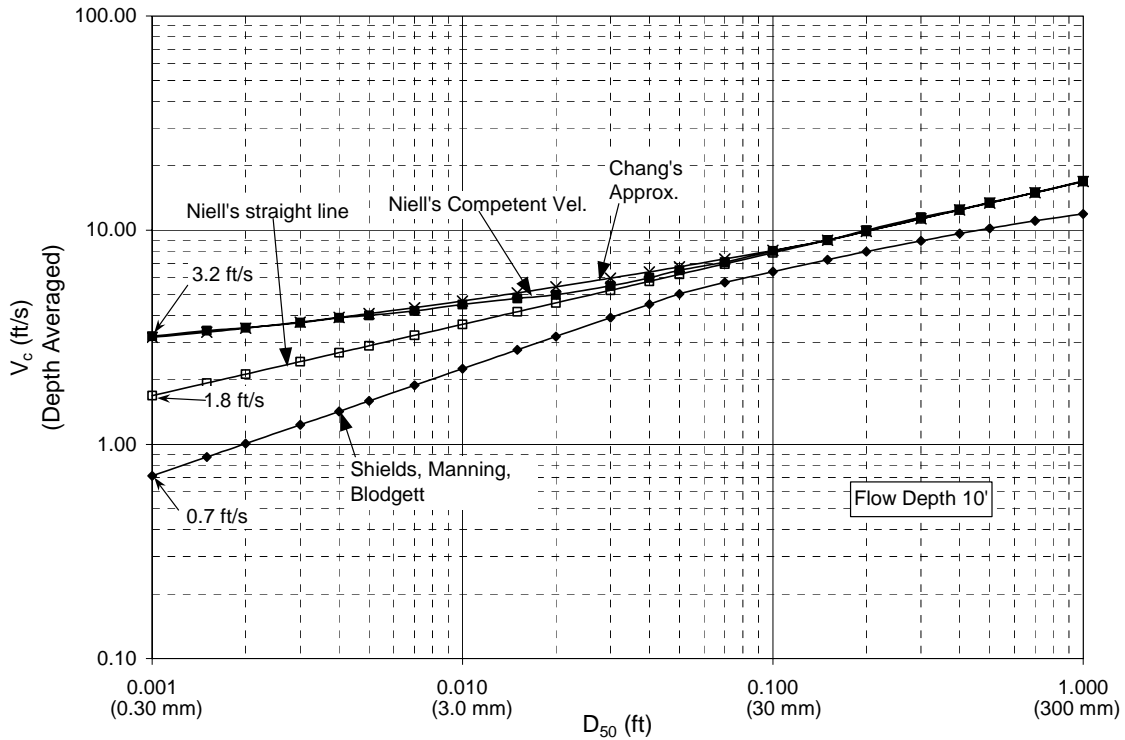
$$V_c = 1.49 * 2.65D_{50}^{1/2} \sqrt{g} \quad \text{for } 185 < \frac{y_2}{D_{50}} < 30,000 \quad (27)$$

Note: $\frac{K_{UM}}{K_{UB}} = 1.49$, regardless of units.

Equation 27 is dimensionally homogenous and does not require a units conversion.

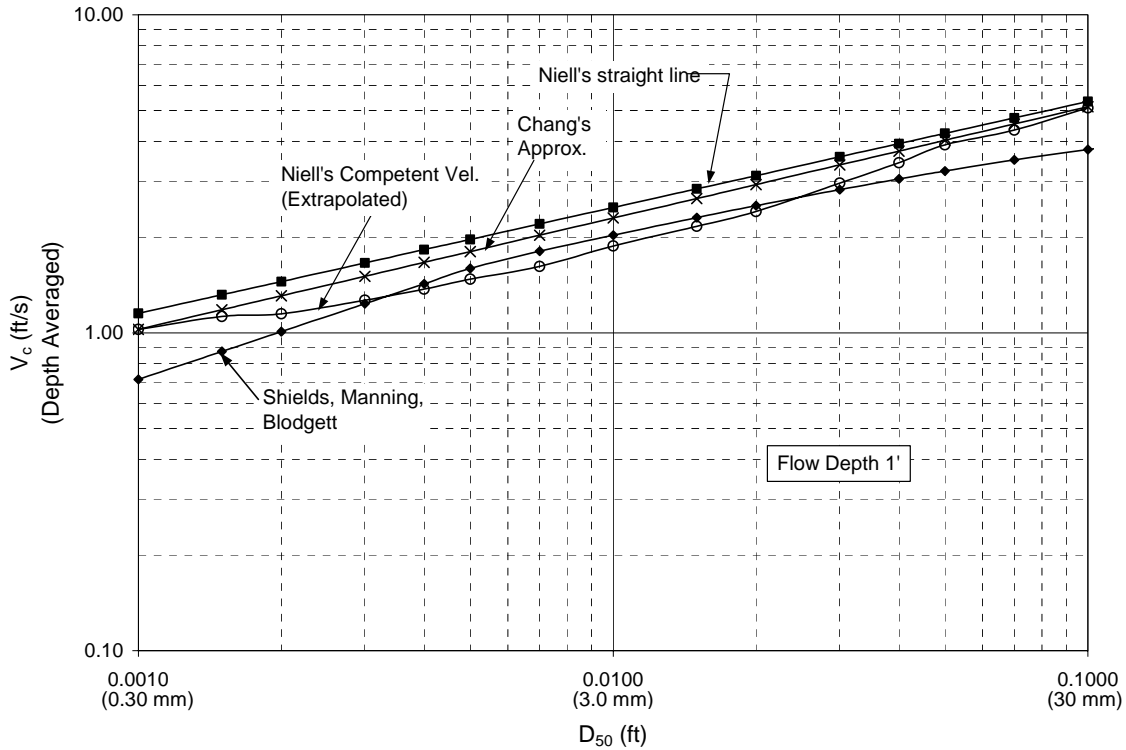
Combined Competent Velocity Curves

To give an overview of how the different competent (critical) velocity methods behave, the critical velocity equations for various particle sizes were plotted for 3- and 0.305-m (10- and 1.0-ft) flow depths (figures 20 and 21). Comparing the two plots, the SMB velocity curve drifts away from Chang's approximation and Niell's competent velocity curve for the 3-m (10-ft) flow depth. For a flow depth of 0.305 m (1 ft), this is not the case, which confirms both methods for critical velocity estimation since the experiments were performed in this flow-depth range.



1 ft = 0.305 m

Figure 20. Combined competent velocity curves for a flow depth of 3 m (10 ft).



1 ft = 0.305 m

Figure 21. Combined competent velocity curves for a flow depth of 0.3 m (1.0 ft).

SCOUR PROTECTION TASK: RIPRAP ANALYSIS

Many researchers have developed critical conditions based on average velocity. Ishbash⁽⁸⁾ presented an equation that can be expressed as:

$$N_{SC} = E \tag{28}$$

Ishbash described two critical conditions for riprap stability. For loose stones where no movement occurs, N_{SC} is expressed as:

$$N_{SC} = \frac{V_{min}^2}{[2g D_{50} (SG - 1)]} \tag{29}$$

$$E = 0.86$$

For loose stones allowed to roll until they become “seated”, N_{SC} is expressed as:

$$N_{SC} = \frac{V_{max}^2}{[2g D_{50} (SG - 1)]} \tag{30}$$

$$E = 1.44$$

where:

N_{SC}	=	computed sediment number for distributed flow
V_{min}	=	minimum velocity that will remove the loose stones lying on top of the fill, ft/s
V_{max}	=	maximum velocity that will roll out the stones lying among the others on the slope, ft/s
g	=	acceleration of gravity
D_{50}	=	diameter of riprap
SG	=	specific gravity of riprap
E	=	constant

Equation 30 for riprap that will just begin to roll can be written as equation 31. For the culvert experiments, we represented the effective velocity (V_{eff}) in terms of an empirical multiplier as indicated by equation 32, which is substituted into equation 31 to yield equation 33.

$$D_{50} = 0.69 \frac{V_{eff}^2}{2g(SG-1)} \quad (31)$$

$$V_{eff} = K_{RIP} V_R \quad (32)$$

$$K_{RIP} = \frac{1.20 \sqrt{2g(SG-1)D_{50}}}{V_R} \quad (33)$$

where:

V_{eff}	=	effective velocity that accounts for turbulence and vorticity in the mixing zone at the upstream corner of a culvert
V_R	=	presumed representative velocity prior to scour in the vicinity of the upstream corner of a culvert
D_{50}	=	diameter of riprap that is expected to be on the verge of failure in the vicinity of the upstream corner of the culvert

Equations 31 through 33 are dimensionally homogeneous and can be used with either system of units as long as they are consistent.

Regression analysis was then performed to derive a function for the coefficient K_{RIP} .

4. RESULTS

SCOUR RESULTS

Extensive analysis was performed using various combinations of equations for resultant velocity and critical velocity. Figure 22 shows how the experimental data was processed and the different evaluation methods used to derive the adjustment coefficients. This section presents the results using the Maryland DOT (Chang) and GKY methods for representative velocity and critical velocity, and the combination that yielded the best results.

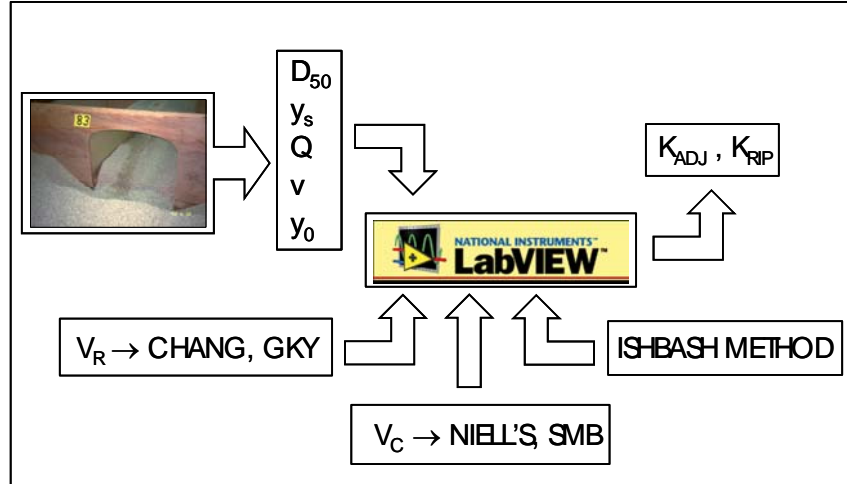


Figure 22. Post-processing: Data analysis flow chart.

The regression analysis was performed for two sets of data: data for the vertical face and data for the wingwall entrances. Separate equations were derived for the two data sets; however, we determined that the two equations could be combined into one general equation by incorporating an entrance coefficient (K_{WW}) to account for the streamlining effects of the wingwalls. Equation 34 is the general expression for the maximum depth to be expected at the upstream corners of a bottomless culvert with no upstream sediment being transported into the scour hole.

$$y_{\max} = K_{WW} K_{ADJ} \frac{V_R}{V_C} y_0 \quad (34)$$

where:

- K_{WW} = wingwall entrance coefficient
- K_{ADJ} = empirical adjustment factor to account for turbulence and vorticity at the upstream corner of the culvert derived from regression analysis

We used R^2 and MSE to indicate which combinations of representative velocity, critical velocity, and independent regression variables worked best for this data.

Maryland DOT (Chang) Method for Representative Velocity and Critical Velocity

Four different independent regression variables were tested for the Maryland DOT method. One of these, the Froude number (N_F) (originally the Chang method), was compared to K_{ADJ} using three different regression methods: linear, second order, and quadratic. The linear regression gave R^2 values of 0.22 for the vertical face data and 0.10 for the wingwall data (figures 23 and 24, respectively).

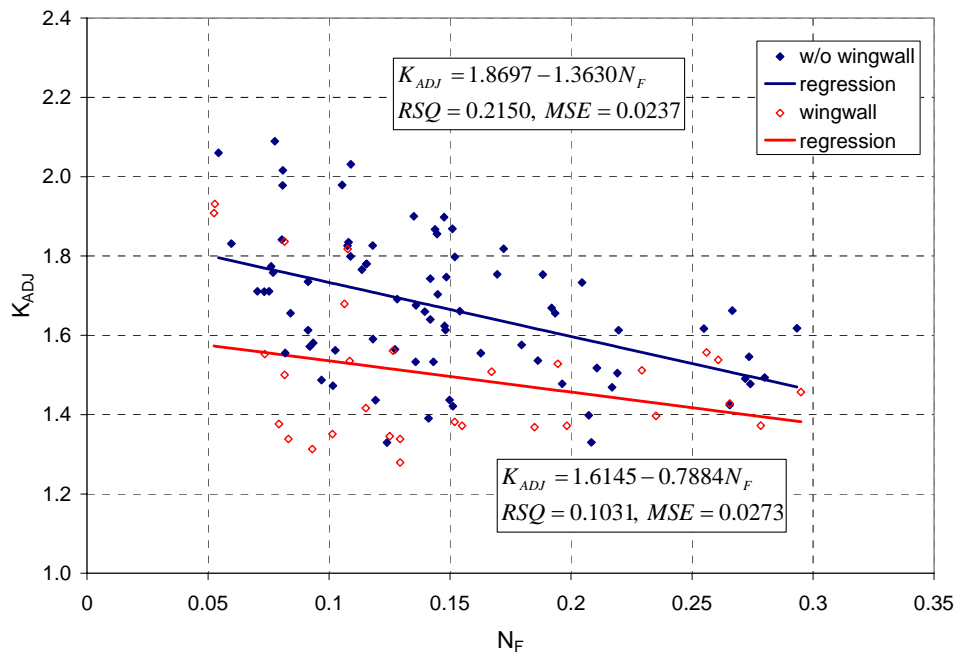


Figure 23. Maryland DOT's (Chang's) resultant velocity with Chang's approximation equation and local scour ratio as a function of the Froude number, using a linear regression.

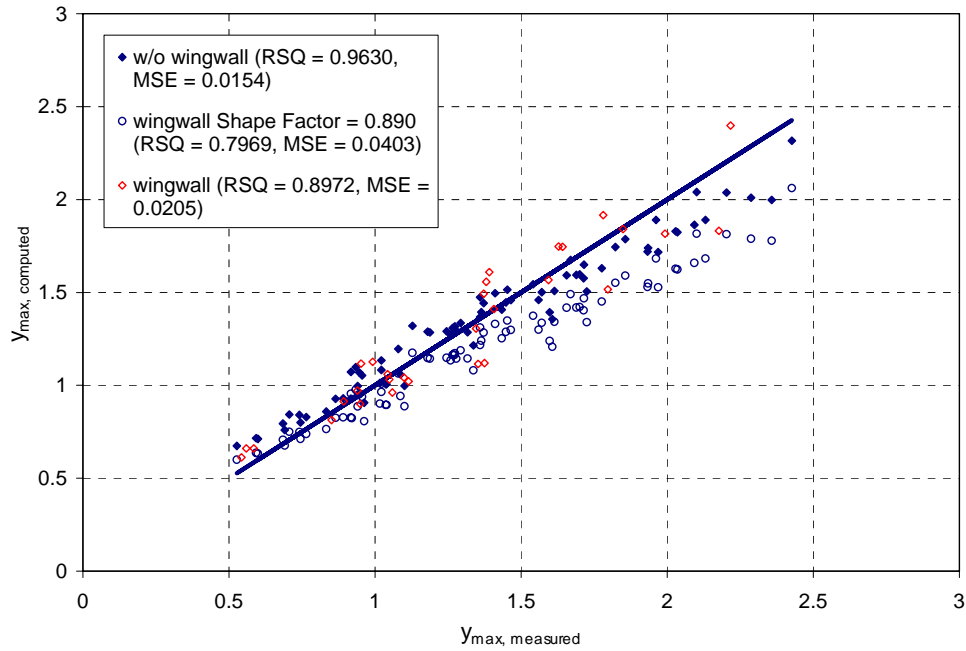


Figure 24. Measured and computed data with and without wingwalls, based on figure 23 regression.

Incorporating the adjustment function from figure 23 leads to the general equation:

$$y_{\max} = K_{ww} (1.8697 - 1.3630 N_F) \frac{V_R}{V_C} y_0 \quad (35)$$

where:

- $K_{ww} = 1.0$ for vertical face entrances
- $= 0.89$ for wingwall entrances

The Froude number (N_F) with a second order regression gave R^2 values of 0.35 for the vertical face data and 0.28 for the wingwall data (figures 25 and 26, respectively).

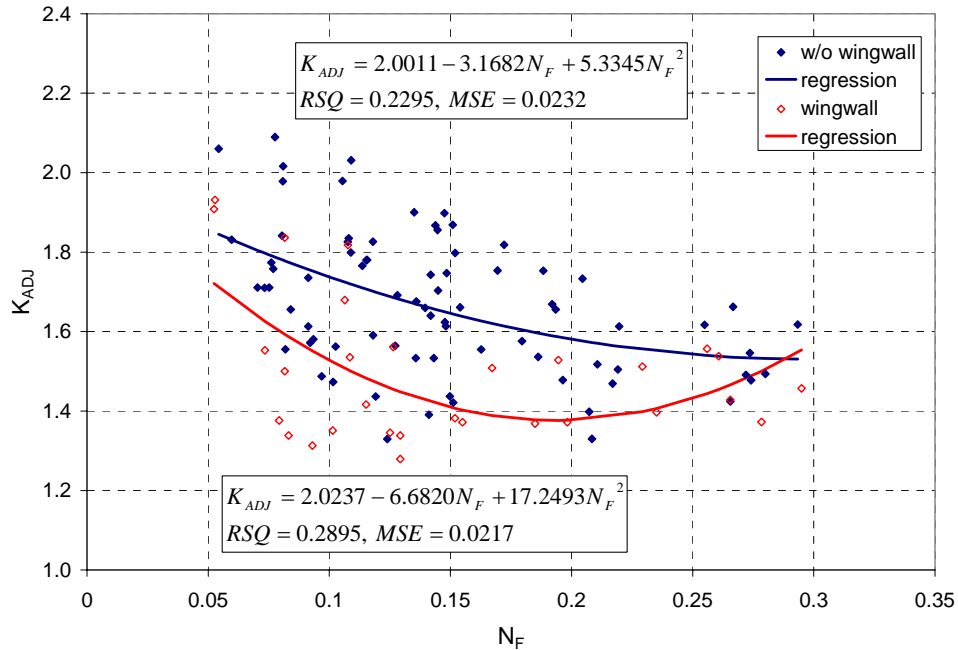


Figure 25. Maryland DOT's (Chang's) resultant velocity with Chang's approximation equation for critical velocity and local scour ratio as a function of the Froude number, using a second order regression.

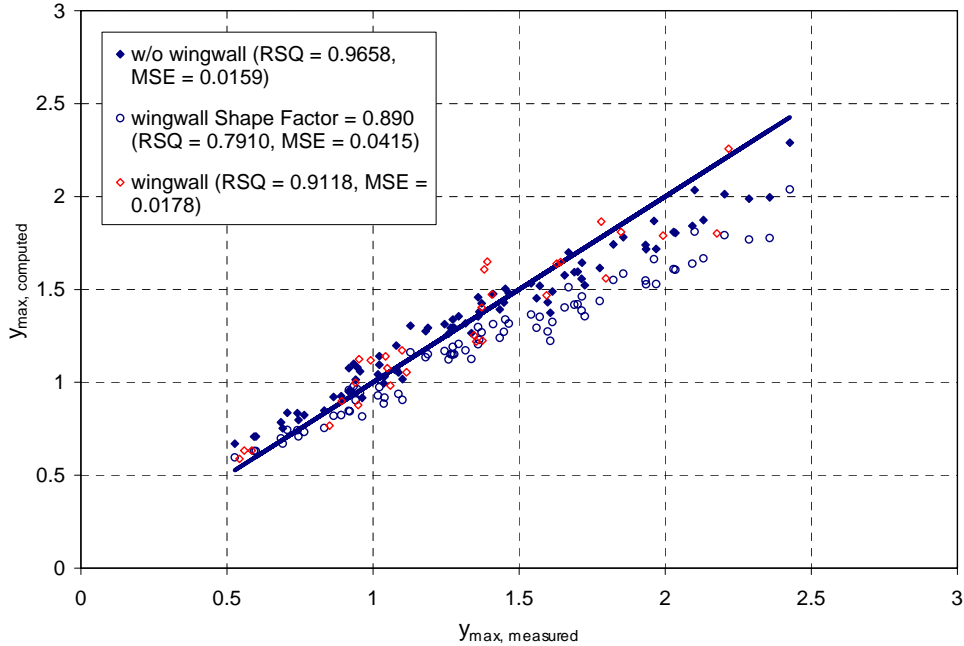


Figure 26. Measured and computed data with and without wingwalls, based on figure 25 regression.

Incorporating the adjustment function from figure 25 leads to the general equation:

$$y_{\max} = K_{ww} (2.0011 - 3.1682 N_F + 5.3345 N_F^2) \frac{V_R}{V_C} y_0 \quad (36)$$

where:

$K_{ww} = 1.0$ for vertical face entrances
 $= 0.89$ for wingwall entrances

The Froude number (N_F) with a quadratic regression gave R^2 values of 0.15 for the vertical face data and 0.06 for the wingwall data (figures 27 and 28, respectively).

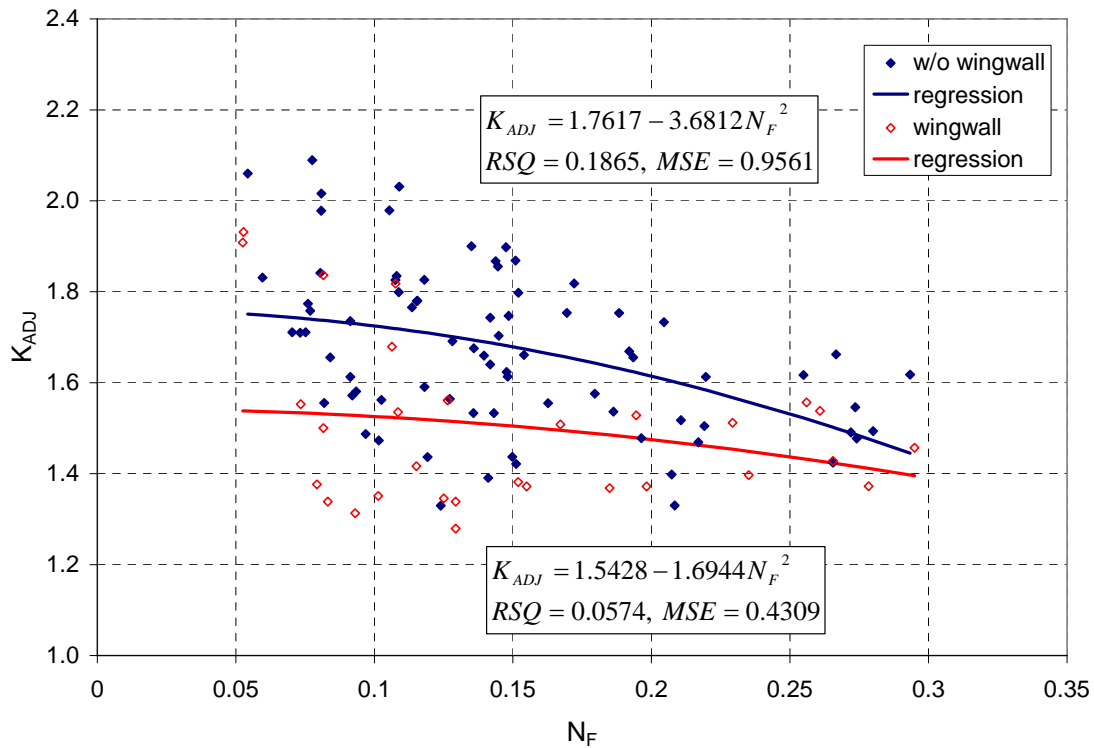


Figure 27. Maryland DOT's (Chang's) resultant velocity with Chang's approximation for critical velocity and local scour ratio as a function of the Froude number, using a linear regression.

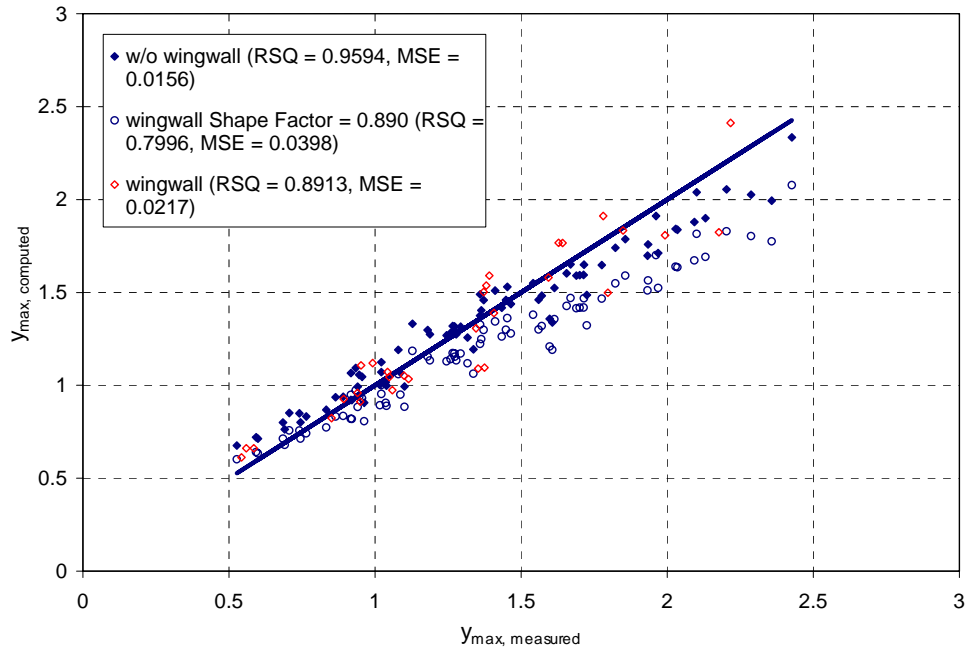


Figure 28. Measured and computed data with and without wingwalls, based on figure 27 regression.

Incorporating the adjustment function from figure 27 leads to the general equation:

$$y_{max} = K_{ww} (1.7617 - 3.6812 N_F^2) \frac{V_R}{V_C} y_0 \quad (37)$$

where:

- $K_{ww} = 1.0$ for vertical face entrances
- $= 0.89$ for wingwall entrances

Using the approach flow area that is blocked by the embankments on one side of the channel over the squared flow depth as the independent regression variable yielded R^2 values of 0.004 for the vertical face data and 0.08 for the wingwall data (figures 29 and 30, respectively).

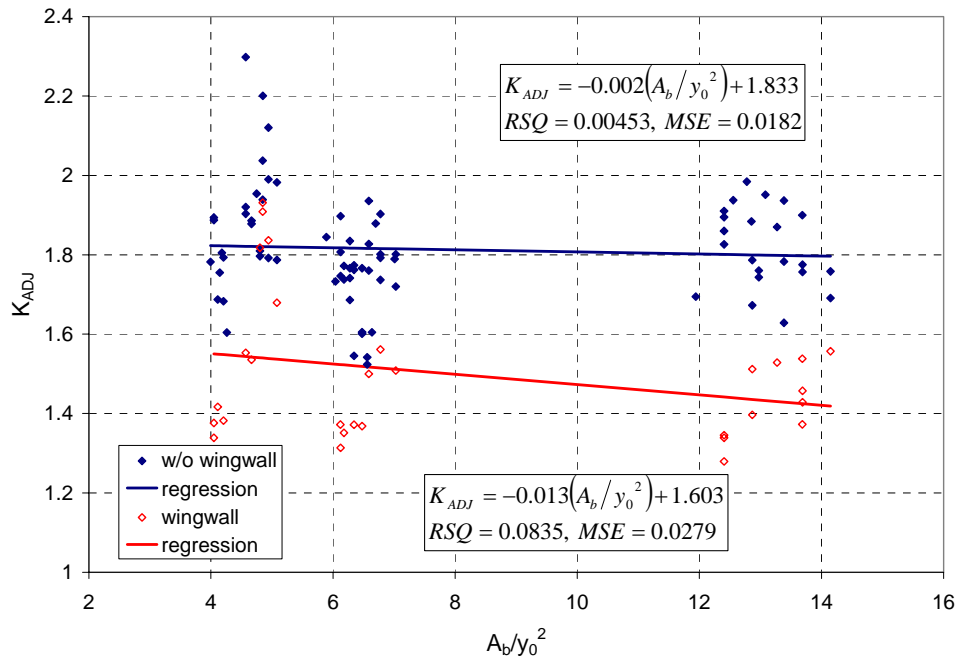


Figure 29. Maryland DOT's (Chang's) resultant velocity with Chang's approximation for critical velocity and local scour ratio as a function of the blocked area over the squared flow depth.

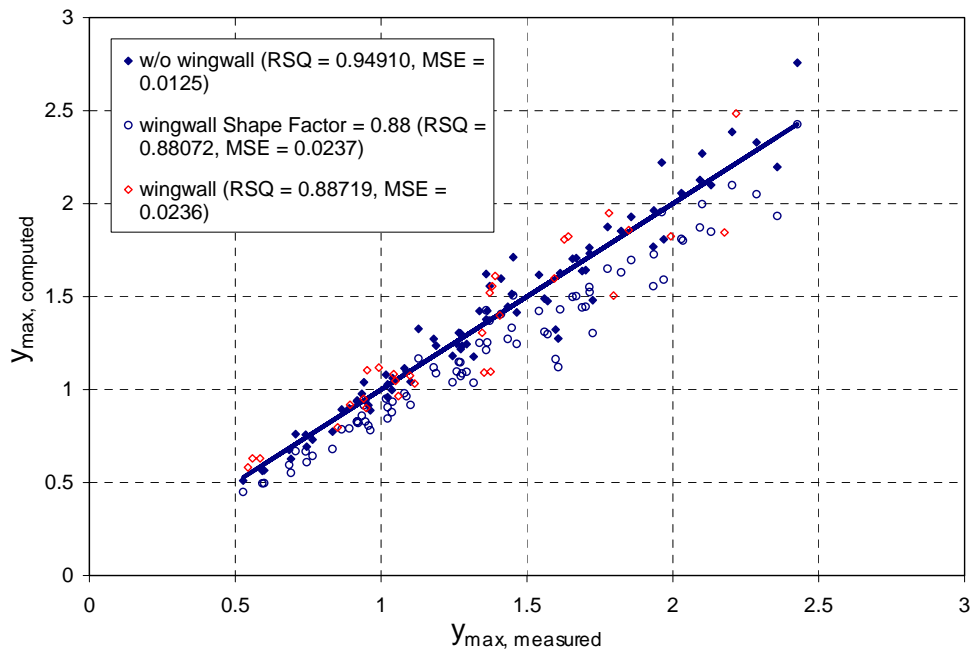


Figure 30. Measured and computed data with and without wingwalls, based on figure 29 regression.

Incorporating the adjustment function from figure 29 leads to the general equation:

$$y_{\max} = K_{WW} \left(1.833 - 0.002 \frac{A_{\text{blocked}}}{y_0^2} \right) \frac{V_R}{V_C} y_0 \quad (38)$$

where:

K_{WW} = 1.0 for vertical face entrances
 = 0.88 for wingwall entrances

The third independent regression variable tested was the approach flow area that is blocked by the embankments on one side of the channel over the squared computed equilibrium depth, resulting in R^2 values of 0.29 for the vertical face data and 0.11 for the wingwall data (figures 31 and 32, respectively).

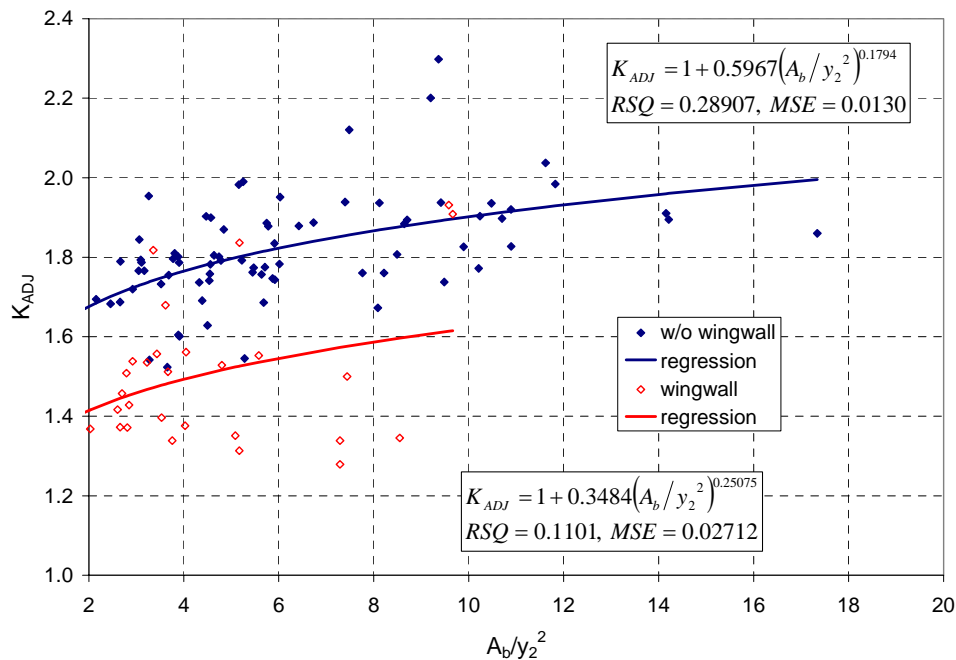


Figure 31. Maryland DOT's (Chang's) resultant velocity with Chang's approximation for critical velocity and local scour ratio as a function of the blocked area over the squared computed equilibrium depth.

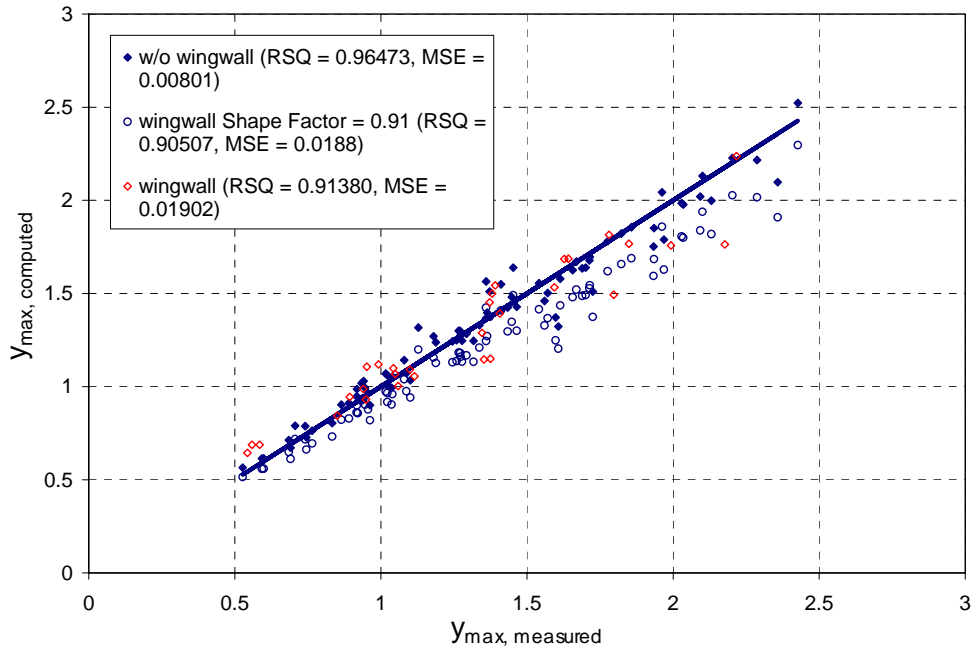


Figure 32. Measured and computed data with and without wingwalls, based on figure 31 regression.

Incorporating the adjustment function from figure 31 leads to the general equation:

$$y_{max} = K_{WW} \left(1.0 + 0.5967 \left(\frac{A_{blocked}}{y_2^2} \right)^{0.1794} \right) \frac{V_R}{V_C} y_0 \quad (39)$$

where:

- $K_{WW} = 1.0$ for vertical face entrances
- $= 0.91$ for wingwall entrances

The fourth independent regression variable tested was the blocked discharge normalized by the acceleration of gravity (g) and the computed equilibrium depth. The R^2 values were 0.07 for the vertical face data and 0.002 for the wingwall data (figures 33 and 34, respectively).

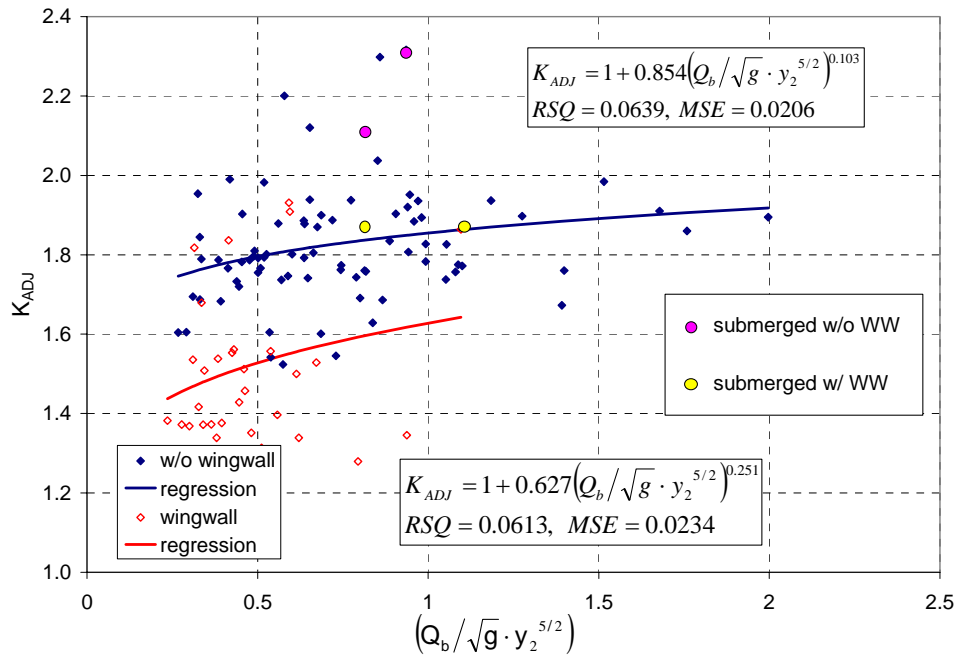


Figure 33. Maryland DOT's (Chang's) resultant velocity with Chang's approximation equation and local scour ratio as a function of the blocked discharge normalized by the acceleration of gravity (g) and the computed equilibrium depth.

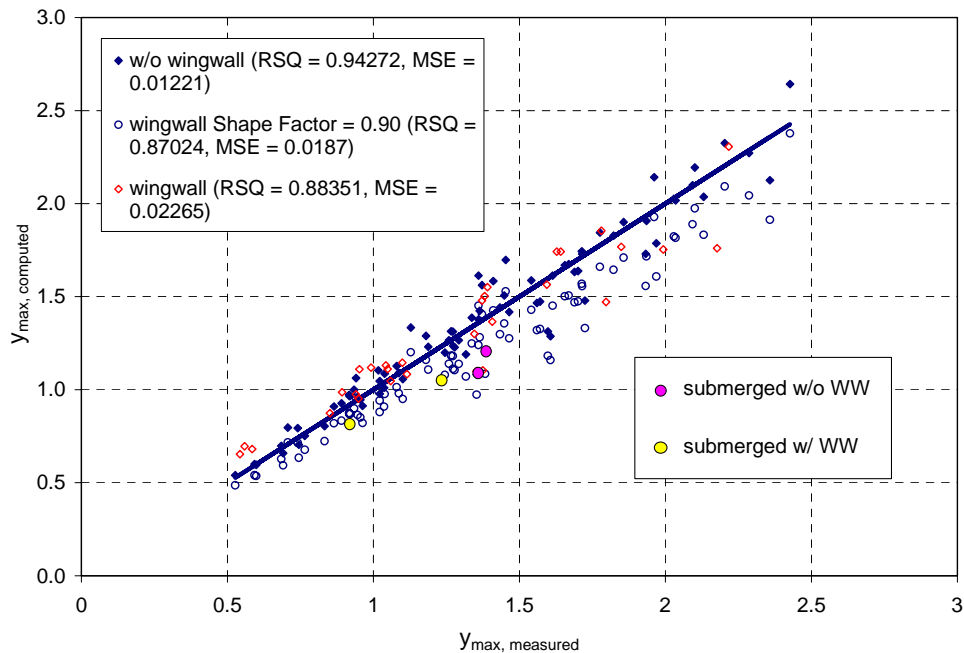


Figure 34. Measured and computed data with and without wingwalls, based on figure 33 regression.

Using the adjustment function from figure 33 gives the general equation:

$$y_{\max} = K_{ww} \left(1.0 + 0.854 \left(\frac{Q_{\text{blocked}}}{\sqrt{g} y_2^{5/2}} \right)^{0.103} \right) \frac{V_R}{V_C} y_0 \quad (40)$$

where:

K_{ww} = 1.0 for vertical face entrances
= 0.89 for wingwall entrances

Table 1 below gives an overview for the tested independent regression variables and R^2 values using the Maryland DOT (Chang) method for representative velocity and critical velocity.

Table 1. Independent regression variables and R² values using the Maryland DOT (Chang) method.

Maryland DOT (Chang) Method for V _R and V _C	R ² Regression	R ² Meas. vs. Comp.	Equation No.
$K_{ADJ} = 1.8697 - 1.3630N_F$	0.2150	0.9630	(41)
$K_{ADJ} = 2.0011 - 3.1682N_F + 5.3345N_F^2$	0.2295	0.9658	(42)
$K_{ADJ} = 1.7617 - 3.6812N_F^2$	0.1865	0.9594	(43)
$K_{ADJ} = 1.833 - 0.002 \frac{A_{blocked}}{y_0^2}$	0.0045	0.9491	(44)
$K_{ADJ} = 1.0 + 0.5967 \left(\frac{A_{blocked}}{y_2^2} \right)^{0.1794}$	0.2891	0.9647	(45)
$K_{ADJ} = 1.0 + 0.854 \left(\frac{Q_{blocked}}{\sqrt{g} y_2^{5/2}} \right)^{0.103}$	0.0639	0.9427	(46)

GKY Method for Representative Velocity and Maryland DOT (Chang) Method for Critical Velocity

Two different independent regression variables were examined for this combination. Again, the approach flow area that is blocked by the embankments on one side of the channel over the squared flow depth was used as the independent regression variable, which gave R² values of 0.00002 for the vertical face data and 0.05 for the wingwall data (figures 35 and 36, respectively).

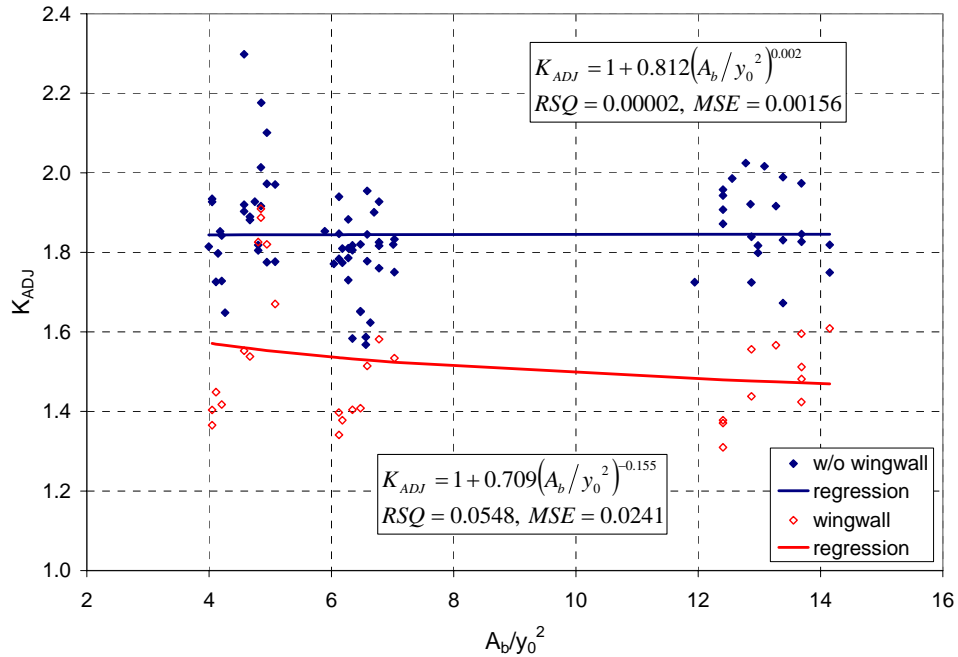


Figure 35. GKY’s resultant velocity with Chang’s approximation equation for the critical velocity and local scour ratio as a function of the blocked area over the squared flow depth.

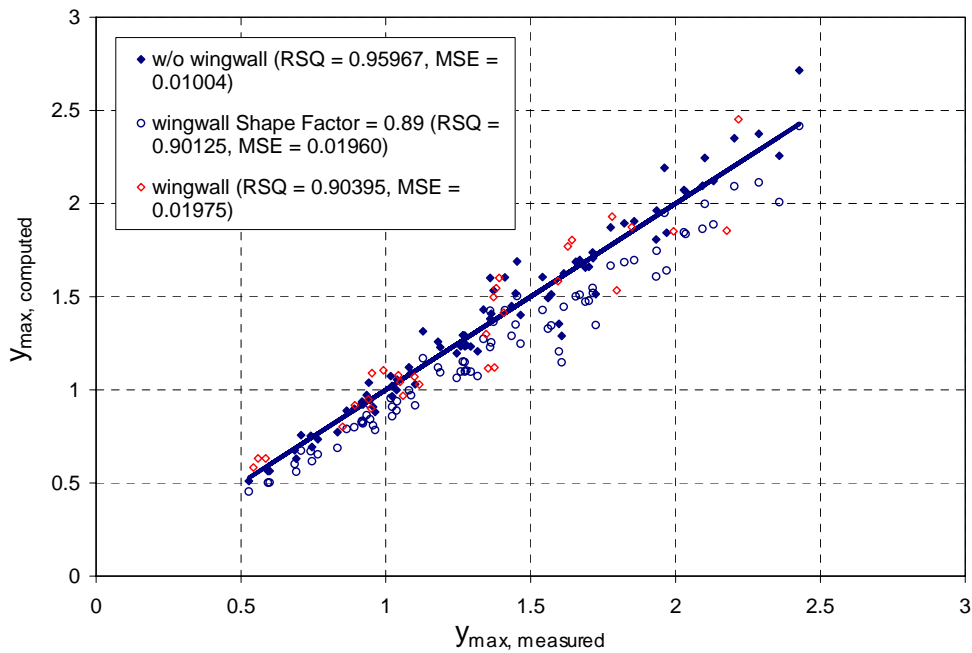


Figure 36. Measured and computed data with and without wingwalls, based on figure 37 regression.

The general equation can be formulated by inserting K_{ADJ} from figure 35:

$$y_{\max} = K_{WW} \left(1.0 + 0.812 \left(\frac{A_{\text{blocked}}}{y_0^2} \right)^{0.002} \right) \frac{V_R}{V_C} y_0 \quad (47)$$

where:

K_{WW} = 1.0 for vertical face entrances
= 0.89 for wingwall entrances

The second independent regression variable tested for this combination was the blocked area over the squared computed equilibrium depth. The R^2 values were 0.30 for the vertical face data and 0.06 for the wingwall data (figures 37 and 38, respectively).

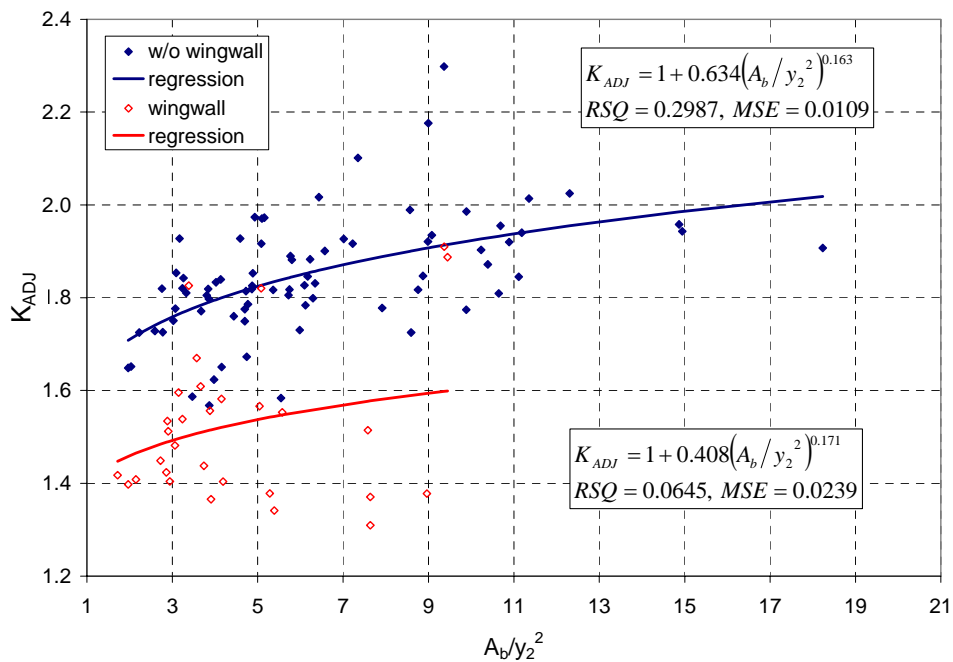


Figure 37. GKY's resultant velocity with Chang's approximation equation for the critical velocity and local scour ratio as a function of the blocked area over the squared computed equilibrium depth.

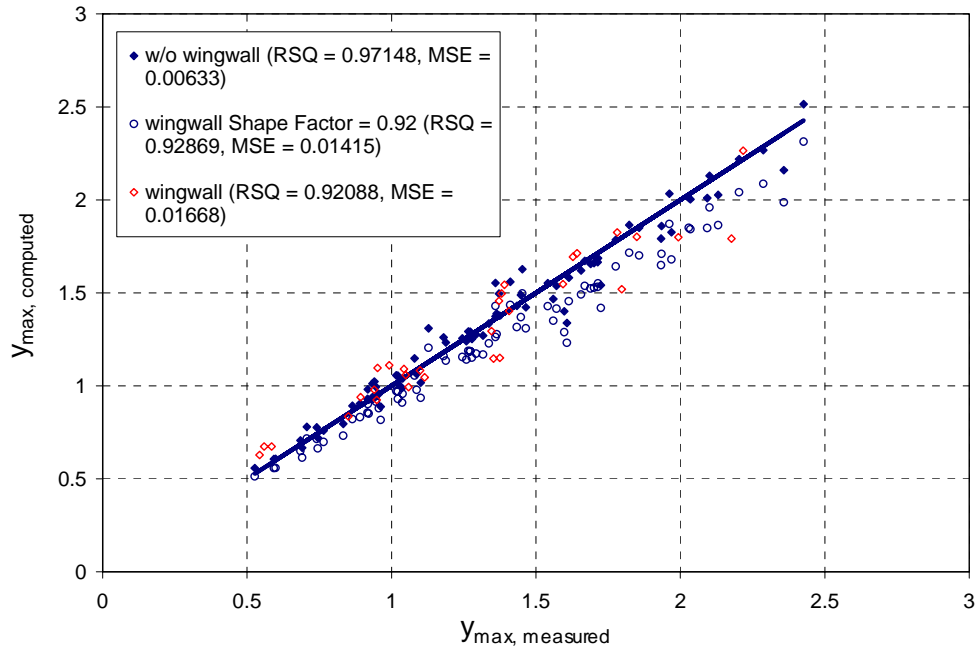


Figure 38. Measured and computed data with and without wingwalls, based on figure 37 regression.

Incorporating the adjustment function from figure 37 leads to the general equation:

$$y_{\max} = K_{ww} \left(1.0 + 0.634 \left(\frac{A_{\text{blocked}}}{y_2^2} \right)^{0.163} \right) \frac{V_R}{V_C} y_0 \quad (48)$$

where:

K_{ww} = 1.0 for vertical face entrances
= 0.92 for wingwall entrances

Table 2 gives an overview for the tested independent regression variables and R^2 values using the GKY method for representative velocity and the Maryland DOT (Chang) method for critical velocity.

Table 2. Independent regression variables and R^2 values using the GKY and Maryland DOT (Chang) methods.

GKY Method for V_R , Maryland DOT (Chang) Method for V_C	R^2 Regression	R^2 Meas. vs. Comp.	Equation No.
$K_{ADJ} = 1.0 + 0.812 \left(\frac{A_{blocked}}{y_0^2} \right)^{0.002}$	0.00002	0.9596	(49)
$K_{ADJ} = 1.0 + 0.634 \left(\frac{A_{blocked}}{y_2^2} \right)^{0.163}$	0.2987	0.9715	(50)

GKY Method for Representative Velocity and Critical Velocity

Three independent regression variables were tried using the GKY method for representative velocity and the GKY method for critical velocity, which is a combination of the SMB equations. Starting again with the approach flow area that is blocked by the embankments on one side of the channel over the squared flow depth as the independent regression variable results in R^2 values of 0.50 for the vertical face data and 0.41 for the wingwall data (figures 39 and 40, respectively).

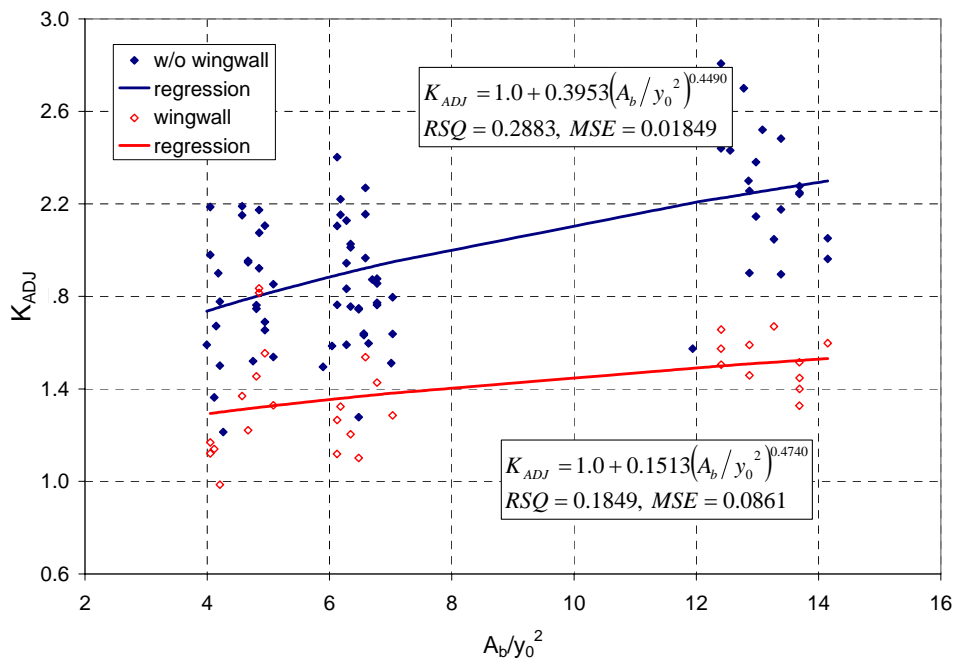


Figure 39. GKY's resultant velocity with the SMB equation for critical velocity and local scour ratio as a function of the blocked area over the squared flow depth.

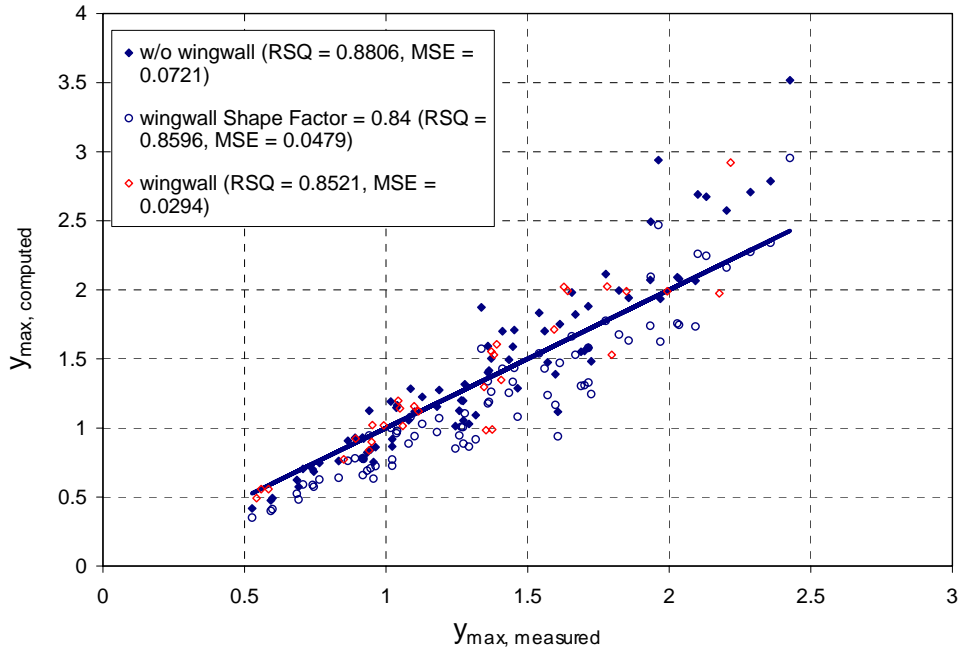


Figure 40. Measured and computed data with and without wingwalls, based on figure 39 regression.

Incorporating the adjustment function from figure 39 leads to the general equation:

$$y_{\max} = K_{WW} \left(1.0 + 0.3953 \left(\frac{A_{\text{blocked}}}{y_0^2} \right)^{0.4490} \right) \frac{V_R}{V_C} y_0 \quad (51)$$

where:

$$\begin{aligned} K_{WW} &= 1.0 \text{ for vertical face entrances} \\ &= 0.87 \text{ for wingwall entrances} \end{aligned}$$

The blocked area over the squared computed equilibrium depth was used as the second independent regression variable. The R^2 values were 0.78 for the vertical face data and 0.38 for the wingwall data (figures 41 and 42, respectively).

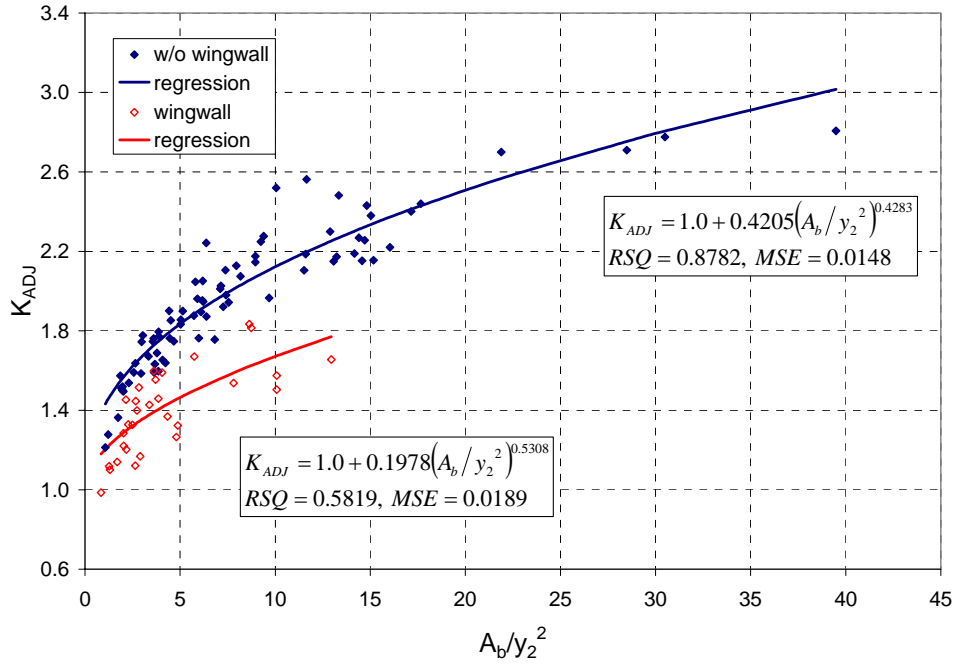


Figure 41. GKY's resultant velocity with the SMB equation for critical velocity and local scour ratio as a function of the blocked area over the squared computed equilibrium depth.

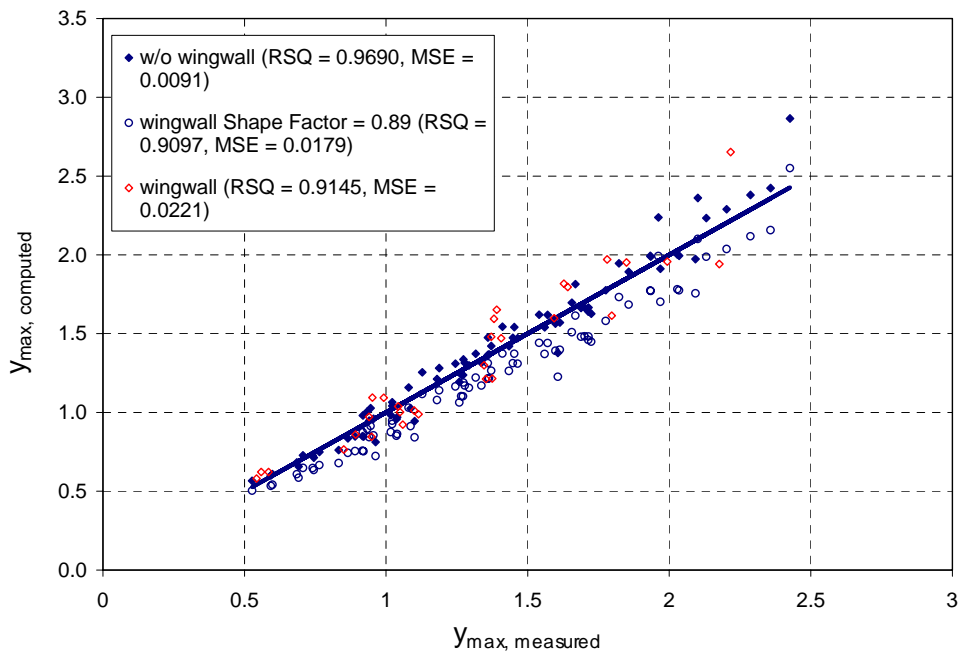


Figure 42. Measured and computed data with and without wingwalls, based on figure 41 regression.

Incorporating the adjustment function from figure 41 leads to the general equation:

$$y_{\max} = K_{ww} \left(1.0 + 0.4205 \left(\frac{A_{\text{blocked}}}{y_2^2} \right)^{0.4263} \right) \frac{V_R}{V_C} y_0 \quad (52)$$

where:

$K_{ww} = 1.0$ for vertical face entrances
 $= 0.89$ for wingwall entrances

Testing the blocked discharge normalized by the acceleration of gravity (g) and the computed equilibrium depth as the independent regression variable yielded the best results. The R^2 values were 0.84 for the vertical face data and 0.47 for the wingwall data (figures 43 and 44, respectively).

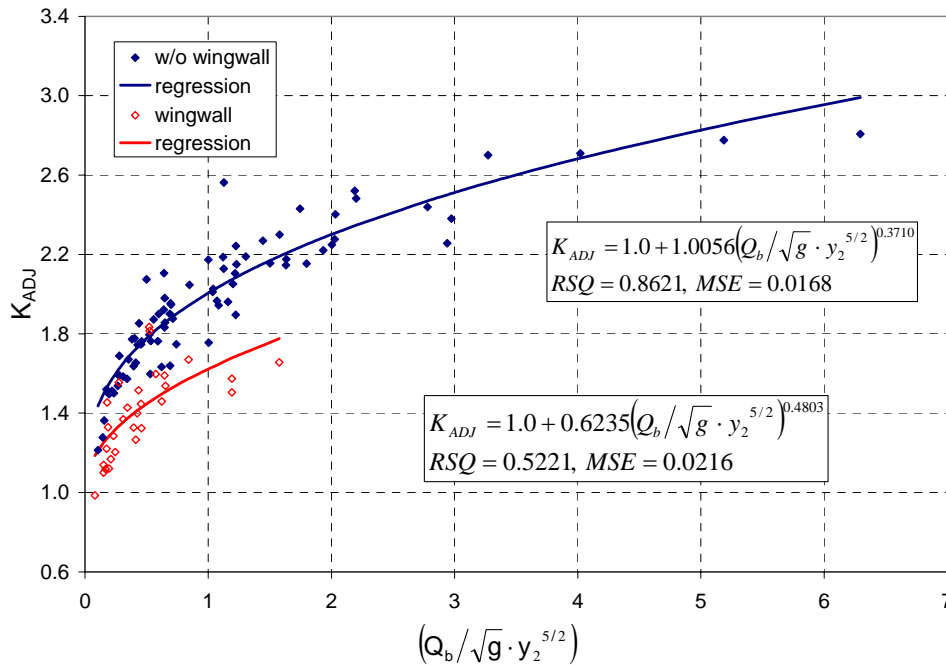


Figure 43. GKY's resultant velocity with the SMB equation for critical velocity and local scour ratio as a function of the blocked discharge normalized by the acceleration of gravity (g) and the computed equilibrium depth.

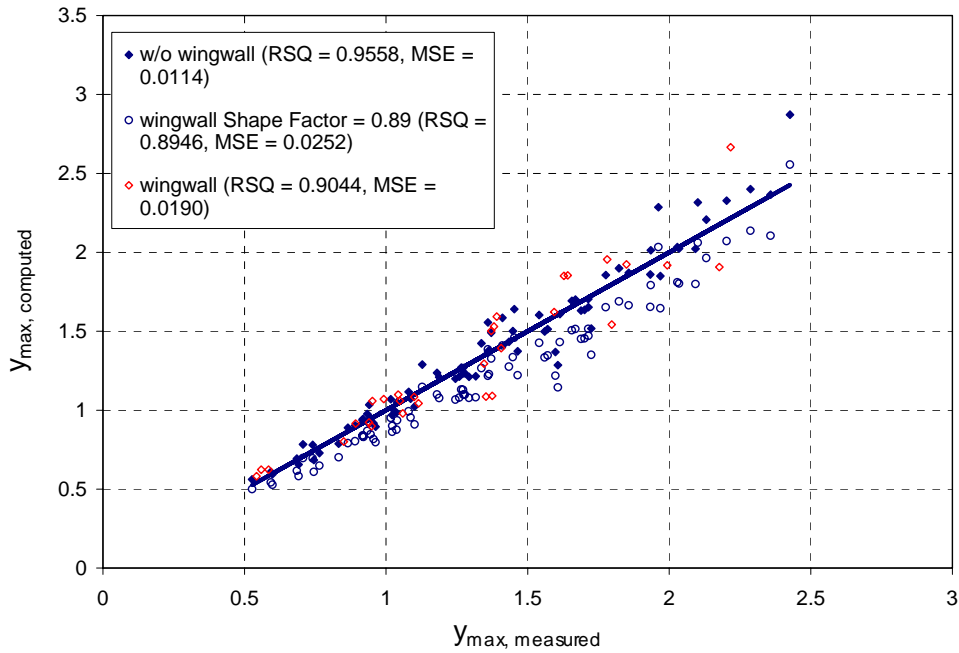


Figure 44. Measured and computed data with and without wingwalls, based on figure 43 regression.

Incorporating the adjustment function from figure 43 leads to the general equation:

$$y_{max} = K_{ww} \left(1.0 + 1.0056 \left(\frac{Q_{blocked}}{\sqrt{g} y_2^{5/2}} \right)^{0.3710} \right) \frac{V_R}{V_C} y_0 \quad (53)$$

where:

$K_{ww} = 1.0$ for vertical face entrances
 $= 0.89$ for wingwall entrances

Table 3 below summarizes the results for the tested independent regression variables and R^2 values using the GKY method for representative velocity and the SMB equation for critical velocity.

Table 3. Independent regression variables and R² values using the GKY method for representative velocity and critical velocity.

GKY Method for V _R , SMB Equations for V _C	R ² Regression	R ² Meas. vs. Comp.	Equation No.
$K_{ADJ} = 1.0 + 0.3953 \left(\frac{A_{blocked}}{y_0^2} \right)^{0.4490}$	0.2883	0.8806	(54)
$K_{ADJ} = 1.0 + 0.4205 \left(\frac{A_{blocked}}{y_2^2} \right)^{0.4263}$	0.8782	0.9690	(55)
$K_{ADJ} = 1.0 + 1.0056 \left(\frac{Q_{blocked}}{\sqrt{g} y_2^{5/2}} \right)^{0.3710}$	0.8621	0.9558	(56)

RIPRAP RESULTS

For the riprap analysis, the Maryland DOT (Chang) and GKY methods for computing representative velocity were used to calculate the effective velocity that accounts for turbulence and vorticity in the mixing zone at the upstream corner of a culvert. Two independent regression variables were used for the blocked area over the squared flow depth and the blocked discharge normalized by the acceleration of gravity (g) and the flow depth to compute the adjustment coefficient K_{RIP}.

Maryland DOT (Chang) Method for Representative Velocity

Using Chang's approximation equation for representative velocity and the approach flow area that is blocked by the embankments on one side of the channel over the squared flow depth to regress the effective velocity gives an R² value of 0.39 (figures 45 and 46).

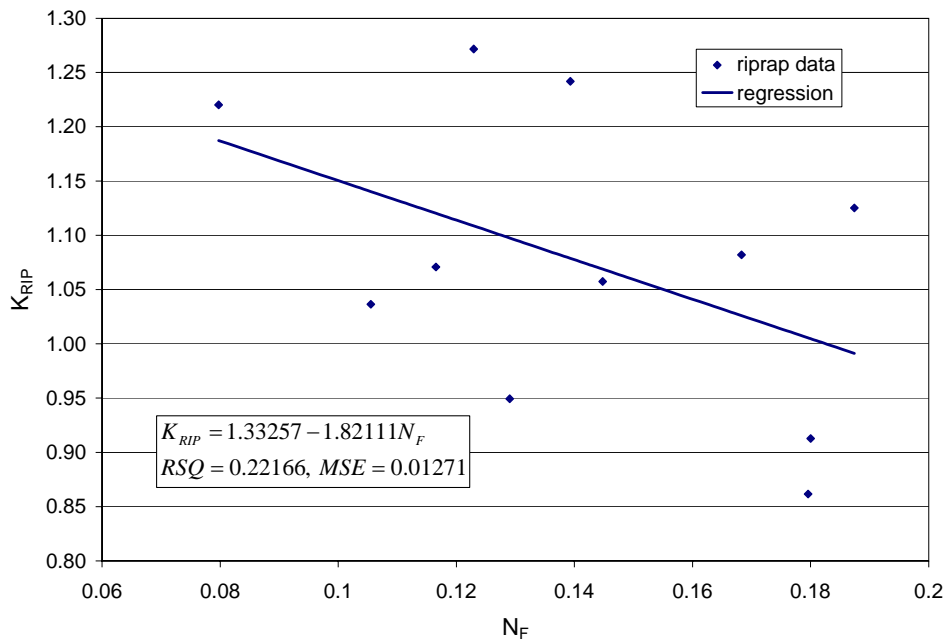


Figure 45. Maryland DOT's (Chang's) resultant velocity and stable riprap size from the Ishbash equation with the blocked area over the squared flow depth as the independent regression variable.

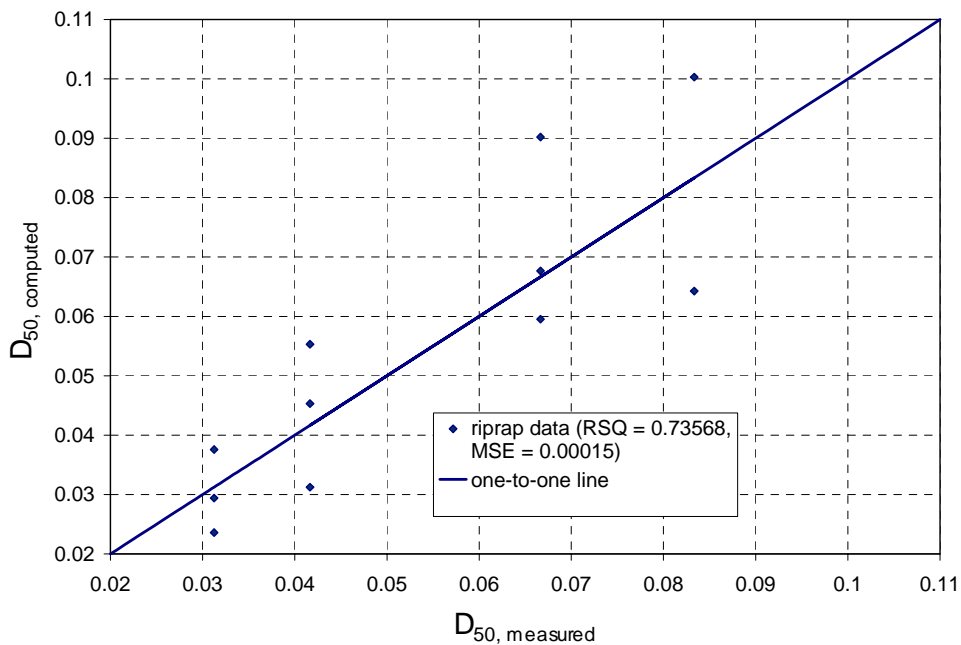


Figure 46. Measured and computed data, based on figure 45 regression.

The expression for sizing riprap at the upstream corners to protect bottomless culvert footings from scour is:

$$D_{50} = 0.69 \frac{(K_{RIP} V_R)^2}{2g(SG-1)} \quad (57)$$

where

$$K_{RIP} = 1.3326 - 1.8211 * N_F \quad (58)$$

from figure 45.

Testing the blocked discharge normalized by the acceleration of gravity (g) and the flow depth as the independent regression variable leads to a regression coefficient, R^2 , value of 0.036 (figures 47 and 48).

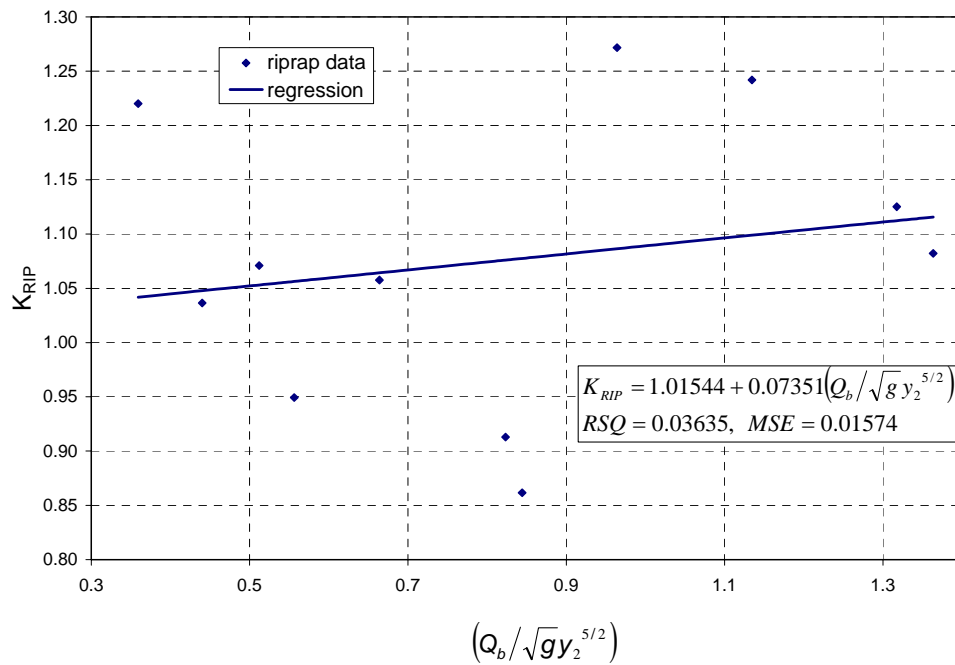


Figure 47. Maryland DOT's (Chang's) resultant velocity and stable riprap size from the Ishbash equation with the blocked discharge normalized by the acceleration of gravity (g) and the flow depth as the independent regression variable.

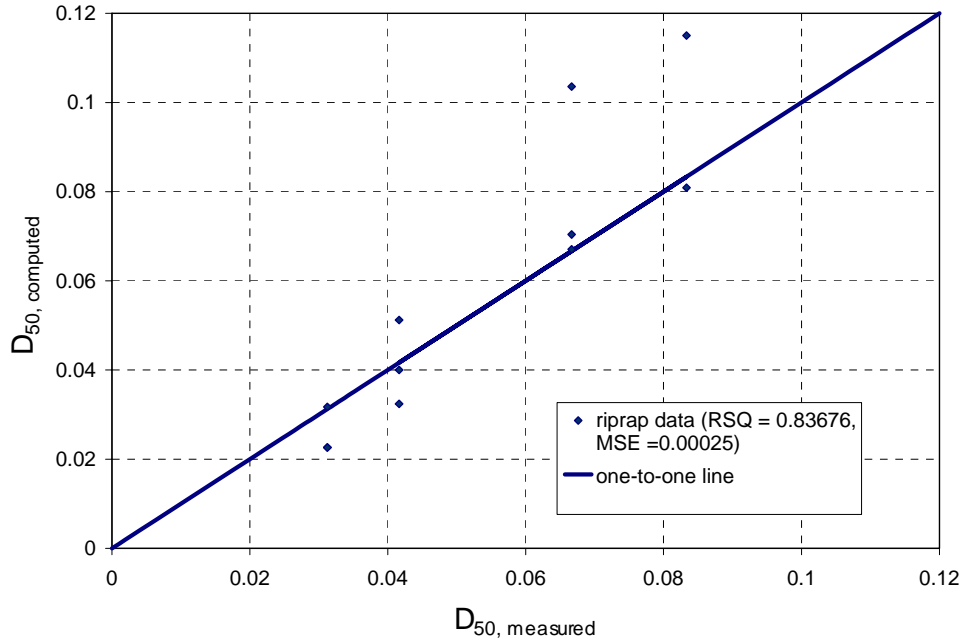


Figure 48. Measured and computed data, based on figure 47 regression.

According to figure 47, the adjustment function for K_{RIP} is:

$$K_{RIP} = 1.0154 + 0.0735 \left(\frac{Q_{blocked}}{\sqrt{g} y_0^{5/2}} \right) \quad (59)$$

Equation 59 can be substituted into equation 57 for the expression for sizing riprap.

Table 4 gives an overview of the tested independent regression variables and R^2 values using Maryland DOT's (Chang's) representative velocity equations.

Table 4. Independent regression variables and R^2 values using the Maryland DOT (Chang) method for representative velocity.

Maryland DOT (Chang) Method for V_R	R^2 Regression	R^2 Meas. vs. Comp.	Equation No.
$K_{RIP} = 1.3326 - 1.8211 * N_F$	0.2217	0.7357	(58)
$K_{RIP} = 1.0154 + 0.0735 \left(\frac{Q_{blocked}}{\sqrt{g} y_0^{5/2}} \right)$	0.0363	0.8367	(59)

GKY Method for Representative Velocity

Computing the GKY method for representative velocity and the approach flow area that is blocked by the embankments on one side of the channel over the squared flow depth to determine the effective velocity gives an R^2 value of 0.39 (figures 49 and 50).

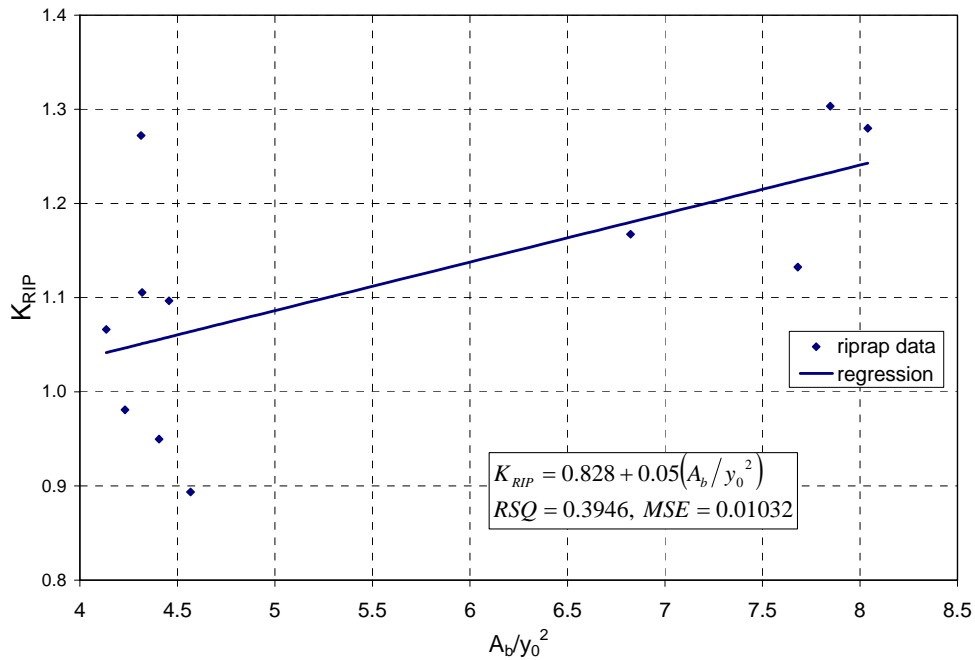


Figure 49. GKY's resultant velocity and stable riprap size from the Ishbash equation with the blocked area over the squared flow depth as the independent regression variable.

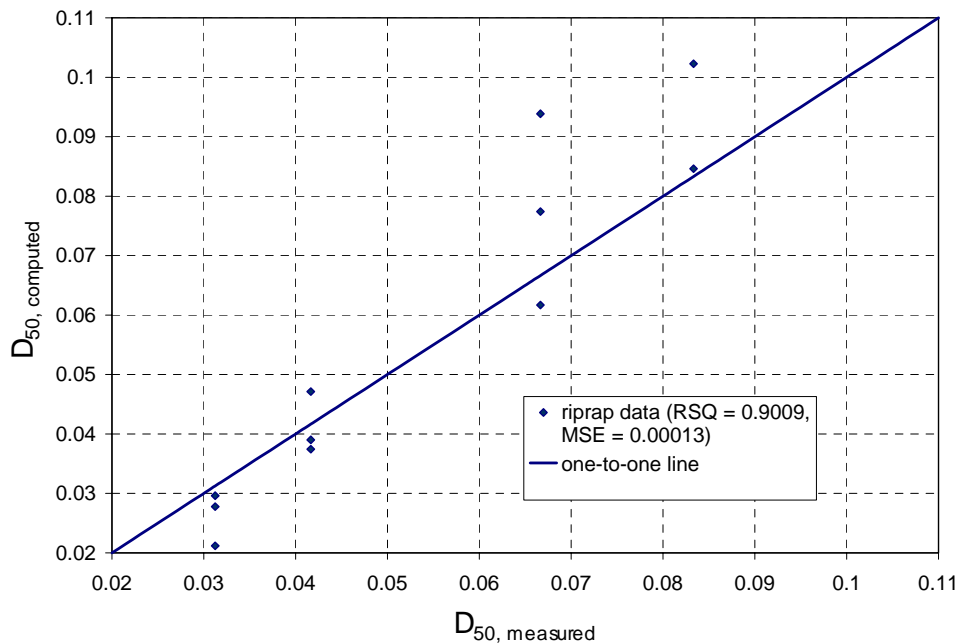


Figure 50. Measured and computed data, based on figure 49 regression.

As indicated in figure 49, the regression analysis leads to:

$$K_{RIP} = 0.828 + 0.05 \left(\frac{A_{blocked}}{y_0^2} \right) \quad (60)$$

Inserting equation 60 into equation 57 yields the expression for sizing riprap.

Finally, the blocked discharge normalized by the acceleration of gravity (g) and the flow depth as the independent regression variable was tested, resulting in a regression coefficient, R^2 , value of 0.04 (figures 51 and 52).

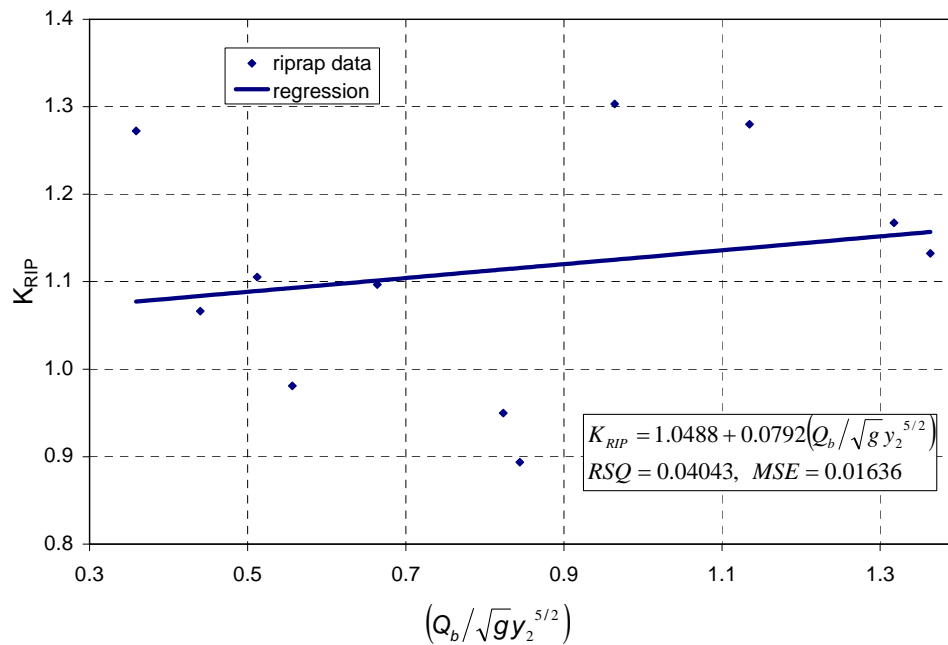


Figure 51. GKY's resultant velocity and stable riprap size from the Ishbash equation with the blocked discharge normalized by the acceleration of gravity (g) and the flow depth as the independent regression variable.

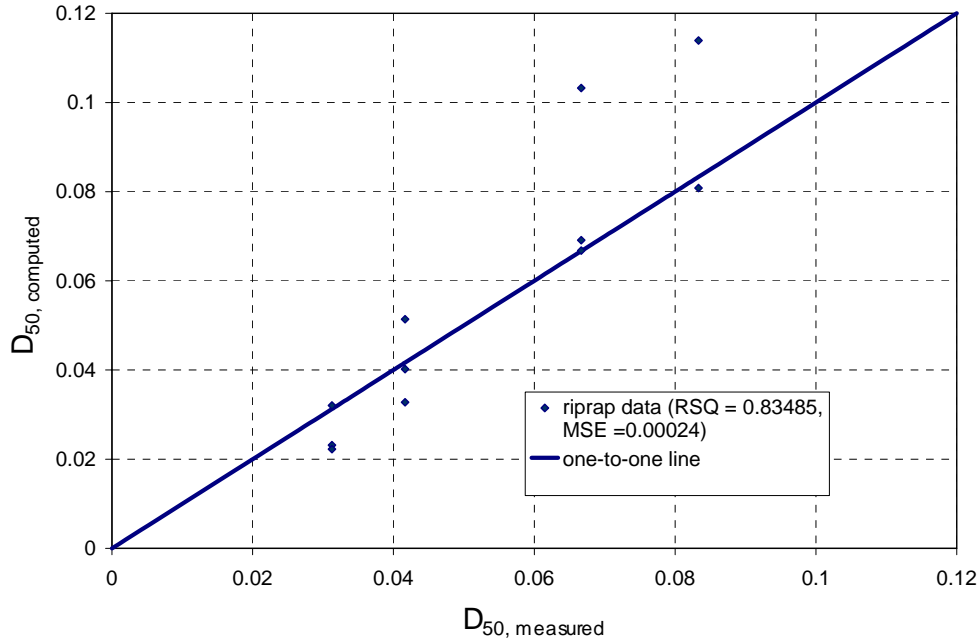


Figure 52. Measured and computed data, based on figure 51 regression.

As shown in figure 51, the regression coefficient function is:

$$K_{RIP} = 1.048 + 0.079 \left(\frac{Q_{blocked}}{\sqrt{g} y_0^{5/2}} \right) \quad (61)$$

To gain the expression for sizing riprap, equation 61 may be substituted into equation 57. Table 5 is an overview of the computed independent regression variables and their R^2 values when using GKY's representative velocity to account for turbulence and vorticity in the mixing zone at the upstream corner of a culvert.

Table 5. Independent regression variables and R^2 values using the GKY method for representative velocity.

GKY Method for V_R	R^2 Regression	R^2 Meas. vs. Comp.	Equation No.
$K_{RIP} = 0.828 + 0.05 \left(\frac{A_{blocked}}{y_0^2} \right)$	0.3946	0.9009	(60)
$K_{RIP} = 1.048 + 0.079 \left(\frac{Q_{blocked}}{\sqrt{g} y_0^{5/2}} \right)$	0.0404	0.8348	(61)

5. CONCLUSIONS

The abutment scour concept of using the flow distribution at the culvert entrance to compute the primary scour depth component and adjusting that with an empirical factor based on laboratory data appears to be valid for bottomless culverts. The culvert shapes tested in these experiments did not significantly influence the scour; however, the entrance conditions did influence the scour.

Equations are presented to estimate the maximum expected flow depths at the upstream corners of bottomless culverts under clear-water conditions. Equations are also presented to estimate the riprap sizes needed to protect bottomless culvert footings from scour.

Two methods for approximating the initial representative velocity and the critical incipient motion velocity, one proposed by GKY and one proposed by Maryland DOT (Chang), were tested. Either method seemed to work reasonably well for representative velocity. The GKY method for critical velocity seemed to work better for the laboratory data; however, critical velocity is independent of the flow depth by the GKY method and is expected to give unreasonably conservative scour estimates for typical field conditions. Maryland DOT's (Chang's) equations for critical velocity were derived for field conditions with depths of 1.5 m (5 ft) or greater and they had to be extrapolated considerably below that depth to be applied to the laboratory conditions.

The limitations of the experimental setup are much more important than the details of which methods should be used for computing velocities. These results are based on laboratory flume experiments with a flat approach cross section with uniform flow conveyance, which is not typical of field conditions. The experiments were also conducted under clear-water approach flow conditions with no sediment being transported into the culvert. The study should be considered a preliminary investigation of a problem that had not been adequately addressed previously. The authors attempted to present the results in terms of overbank flow rather than geometric variables because it can account for the reduced conveyance that is typical of overbank flow for natural streams. These results have not been tested for field conditions; however, they are offered as initial guidance for field applications. An anticipated next step is that the Maryland SHA will adopt the results as preliminary design guidelines and test them for field sites using engineering judgment to decide if the applications are reasonable.

Additional research could extend and/or improve upon the study results, including:

- Conceptual sediment balance relationships to extend the analysis to live-bed conditions. The authors propose that Laursen's "sediment-in equals sediment-out" logic (that the amount of sediment entering a stream segment must equal the amount of sediment exiting) should apply with reasonable assumptions about flow distributions. An inherent assumption is that the empirical adjustment factors from the clear-water experiments can be applied to live-bed conditions. Live-bed flume experiments with sediment transport in the main channel and clear water (no sediment) in overbank flow are needed to test these assumptions.
- Additional riprap tests to improve the riprap analysis. More data are needed, including experiments with wingwalls.

- Derivation of a safety factor to envelop the experimental riprap data. Engineers often find that they end up using the same class of riprap for a wide range of requirements. A safety factor provides a level of confidence in applying engineering judgment in these situations.
- Fixed-bed experiments to accurately measure initial flow distributions and flow redistribution as it flows through the culvert. One of the problems with moveable-bed experiments is that conditions change as soon as the experiments begin. This information will help validate approximations and determine how the scour depths might diminish and redistribute beyond the culvert entrance. Fixed-bed velocity measurements need to be compared to the 1D approximations and 2D numerical model results to determine if the numerical model flow distribution would be a better platform for developing the regression equations.

6. RECOMMENDED PROCEDURES FOR ESTIMATING MAXIMUM SCOUR FOR BOTTOMLESS CULVERTS

PROCEDURE USING GKY METHOD FOR REPRESENTATIVE VELOCITY AND SMB EQUATION FOR CRITICAL VELOCITY

The GKY method for representative velocity and the SMB equation for critical velocity with the blocked discharge normalized by the acceleration of gravity (g) and the computed equilibrium depth as the independent regression variable gave the best R^2 value, regressing the K_{ADJ} (see equation 3) to compute the maximum scour for the laboratory data. The SMB method for computing critical velocity, however, is independent of the flow depth and produces much lower critical velocities than the other methods for fine particle sizes. This will, in turn, result in overly conservative scour estimates for field situations.

The procedure is:

Step 1: Compute representative velocity using:

$$V_R = \sqrt{V_x^2 + V_y^2} \quad (62)$$

with

$$V_x = \frac{Q}{A_{opening}} \quad (63)$$

and

$$V_y = \frac{Q_{blocked \phi}}{0.43 A_{a\phi}} \quad (64)$$

where:

- V_x = velocity in the flow direction, ft/s
- V_y = velocity orthogonal to the flow direction, ft/s
- $Q_{blocked \phi}$ = approach flow blocked by the embankment on one side of the channel centerline, ft³/s
- $A_{a\phi}$ = total approach flow area on one side of the channel centerline, ft²
- $A_{blocked}$ = approach flow area that is blocked by the embankments on one side of the channel, ft²

Step 2: Determine critical velocity by applying the SMB equations. The Shields Manning equations can be combined to yield:

$$V_C = \frac{K_{UM} 0.28 D_{50}^{1/2} y_2^{1/6}}{n} \quad (65)$$

where:

K_{UM} = 1.0 for SI units or
 1.49 for U.S. customary units
 n = Manning's roughness

Blodgett's equations for average estimates of Manning's n for sand- and gravel-bed channels are:

$$n = \frac{K_{UB} 0.525 y_2^{1/6}}{\sqrt{g} \left[0.794 + 1.85 \text{Log} \left(\frac{y_2}{D_{50}} \right) \right]} \quad \text{for } 1.5 < \frac{y_2}{D_{50}} < 185 \quad (66)$$

$$n = \frac{K_{UB} 0.105 y_2^{1/6}}{\sqrt{g}} \quad \text{for } 185 < \frac{y_2}{D_{50}} < 30,000 \quad (67)$$

where:

g = acceleration of gravity =
 9.81 m/s² for SI units or
 32.2 ft/s² for U.S. customary units
 K_{UB} = 1/1.49 for SI units or
 1.0 for U.S. customary units

Step 3: Calculate y_2 using:

$$y_2 = \frac{V_R y_0}{V_C} \quad (68)$$

Step 4: Use following regression equation to compute K_{ADJ} :

$$K_{ADJ} = 1.0 + \left(\frac{Q_{blocked}}{\sqrt{g} y_2^{5/2}} \right)^{0.37} \quad (69)$$

with

$$Q_{blocked} = Q \frac{A_{blocked}}{A_a} \quad (70)$$

where:

$Q_{blocked}$ = approach flow blocked by the embankment on one side of the channel centerline, ft³/s

A_a = total approach flow area on one side of the channel, ft²
 A_{blocked} = approach flow area that is blocked by the embankments on one side of the channel, ft²

Step 5: Compute maximum scour according to:

$$y_{\text{max}} = K_{ADJ} y_2 \quad (71)$$

PROCEDURE USING MARYLAND DOT (CHANG) METHOD FOR REPRESENTATIVE VELOCITY AND CRITICAL VELOCITY

The recommended procedure is based on using the Maryland DOT (Chang) method for computing both representative velocity and critical velocity. For computing the K_{ADJ} factor, the method using the blocked discharge normalized by the acceleration of gravity (g) and the computed equilibrium depth as the independent regression variable was chosen because it is considered to be more applicable to field situations.

The procedure is:

Step 1: Compute representative velocity using the Maryland DOT (Chang) method:

$$V_R = K_V \left[\frac{Q}{A_{\text{opening}}} \right] \quad (72)$$

with

$$K_V = 1 + 0.8 \left(\frac{w_{\text{opening}}}{w_a} \right)^{1.5} \quad (73)$$

where:

K_V = velocity coefficient to account for flow concentration where side flow converges with main channel flow based on potential flow assumptions
 Q = total discharge through the culvert, ft³/s
 A_{opening} = average flow area within the culvert, ft²
 w_{opening} = average flow width in the culvert, ft
 w_a = width of flow in the approach section, ft

These equations are dimensionally homogeneous and are independent of the system of units as long as they are consistent.

Step 2: Determine critical velocity using the Maryland DOT (Chang) method:

- For $D_{50} > 0.03$ m (0.1 ft):

$$V_C = K_U 11.5 y_2^{1/6} D_{50}^{1/3} \quad (74)$$

where:

y_2 = equilibrium flow depth, m or ft
 D_{50} = sediment size, m or ft
 K_U = 0.55217 for SI units or
 1.0 for U.S. customary units

- For $0.03 \text{ m (0.1 ft)} > D_{50} > 0.0003 \text{ m (0.001 ft)}$:

$$V_C = K_{U1} 11.5 y_2^x D_{50}^{0.35} \quad (75)$$

The exponent x is calculated using equation 13:

$$x = K_{U2} \frac{0.123}{D_{50}^{0.20}} \quad (76)$$

where:

y_2 = equilibrium flow depth, m or ft
 D_{50} = sediment size, m or ft
 K_{U1} = $0.3048^{(0.65-x)}$ for SI units or
 1.0 for U.S. customary units
 x = exponent from equation 13
 K_{U2} = 0.788 for SI units or
 1.0 for U.S. customary units

- For $0.0003 \text{ m (0.001 ft)} > D_{50}$:

$$V_C = K_U \sqrt{y_2} \quad (77)$$

where:

y_2 = equilibrium flow depth, m or ft
 D_{50} = sediment size, m or ft
 K_U = 0.55217 for SI units or
 1.0 for U.S. customary units

Step 3: Calculate y_2 using:

$$y_2 = \frac{V_R y_0}{V_C} \quad (78)$$

Step 4: Use the following regression equation to compute K_{ADJ} :

$$K_{ADJ} = 1.0 + 0.8425 \left(\frac{Q_{blocked}}{\sqrt{g} y_2^{5/2}} \right)^{0.09029} \quad (79)$$

with

$$Q_{blocked} = Q \frac{A_{blocked}}{A_a} \quad (80)$$

where:

$Q_{blocked}$ = approach flow blocked by the embankment on one side of the channel, ft³/s
 A_a = total approach flow area on one side of the channel, ft²
 $A_{blocked}$ = approach flow area that is blocked by the embankments on one side of the channel, ft²

Step 5: Compute maximum scour according to:

$$y_{max} = K_{ADJ} y_2 \quad (81)$$

7. REFERENCES

1. Chang, F., /Maryland DOT. *Maryland SHA Procedure for Estimating Scour at Bridge Abutments Part 2-Clear Water Scour*, ASCE Proceedings of the International Water Resources Engineering Conference held in Memphis, TN, Vol. 1 pp 169-173, 1998.
2. Young K. G., et al./GKY and Associates., Inc. *Testing Abutment Scour Model*, ASCE Proceedings of the International Water Resources Engineering Conference held in Memphis, TN, Vol. 1 pp 180-185, 1998.
3. Sturm, T. W. et al. *Abutment Scour in Compound Channels for Variable Setbacks*, ASCE Proceedings of the International Water Resources Engineering Conference held in Memphis, TN, Vol. 1 pp 180-185, 1998.
4. Niell, C. R. *Guide to Bridge Hydraulics*, University of Toronto Press, Toronto, Canada, 1973
5. Shields, A. *Anwendung der Aehnlichkeitsmechanik und der Turbulenzforschung auf die Geschiebepbewegung*, Mitteilung der Preussischen Versuchsanstalt für Wasserbau und Schiffbau”, Heft 26, Berlin, (In German), 1936.
6. Manning, R. *On the Flow of Water in Open Channels and Pipe*, Institution of Civil Engineers of Ireland, 1890.
7. Blodgett, J. C. *Rock Riprap Design for Protection of Stream Channels Near Highway Structures*, Vol. 1—Hydraulic Characteristics of Open Channels, U.S. Geological Survey, Report 86-4127, Sacramento, California, 1986.
8. Ishbash, S. V. *Construction of Dams By Depositing Rock in Running Water*, Second Congress on Large Dams, Communication No. 3, Washington, D.C. 1936.